

1

2 **Seed morphology and anatomy and its utility in recognizing subfamilies and tribes of**

3 **Zingiberaceae¹**

4

5

6 John C. Benedict^{2,10}, Selena Y. Smith^{2,3}, Margaret E. Collinson⁴, Jana Leong-Škorničková⁵,

7 Chelsea D. Specht⁶, Federica Marone⁷, Xianghui Xiao⁸, and Dilworth Y. Parkinson⁹

8

9 ¹Manuscript received ____; revision accepted ____.

10 ²Dept. of Earth and Environmental Sciences, University of Michigan, Ann Arbor, MI, USA,

11 48109-1005

12 ³Museum of Paleontology, University of Michigan, Ann Arbor, MI, USA, 48109-1079

13 ⁴Dept. of Earth Sciences, Royal Holloway University of London, London, UK, TW20 0EX

14 ⁵Herbarium, Singapore Botanic Gardens, National Parks Board, Singapore, 259569

15 ⁶Dept. of Plant and Microbial Biology, Integrative Biology and the University and Jepson

16 Herbaria, University of California, Berkeley, CA, USA, 94750-2465

17 ⁷Swiss Light Source, Paul Scherrer Institut, 5232 Villigen PSI, Switzerland

18 ⁸Advanced Photon Source, Argonne National Laboratories, Argonne, IL, USA, 60439

19 ⁹Advanced Light Source, Lawrence Berkeley National Labs, Berkeley, CA, USA, 94720

20 ¹⁰Author for correspondence (email: jcbenedi@umich.edu)

21

22 ACKNOWLEDGEMENTS

23 The authors would like to thank A. Reznicek (MICH), W.J. Kress, I. Lopez, and J. Wen (US), W.

24 Friedrich (Aarhus University), and J. Kallunki and S. Sylva (NY) for facilitating access to

25 material that formed part of this study; and M. Andrew, G. Benson-Martin, S. Brown, J.

26 Defontes, J. Dorey, J.L. Fife, S. Joomun, S. Little, A. Pineyro, S. McKechnie, K. Morioka, M.

27 Ng, B. Robson, N. Sheldon, and R. Yockteng for help at the beamlines. This work was supported

28 by a Heliconia Society International award to J.C.B. and National Science Foundation grants

29 DEB 1257080 (S.Y.S) and 1257701 (C.D.S). Research of J.L.S. is supported by National Parks

30 Board, Singapore and the Czech Science Foundation, GAČR P506–14–13541S. A portion of this
31 work was included in the Ph.D. dissertation of J.C.B. mentored by K.B. Pigg, whom J.C.B.
32 would like to thank. The research at TOMCAT beamline at the Swiss Light Source, Paul
33 Scherrer Institut, Villigen, Switzerland received funding from Integrated Infrastructure Initiative
34 (I3) on Synchrotrons and FELs and the European Community's Seventh Framework Programme
35 (FP7/2007–2013) under grant agreement n.°312284 (CALIPSO) through SLS to M.E.C. and
36 S.Y.S. This research used resources of the Advanced Photon Source, a U.S. Department of
37 Energy (DOE) Office of Science User Facility operated for the DOE Office of Science by
38 Argonne National Laboratory under Contract No. DE–AC02–06CH11357. The Advanced Light
39 Source is supported by the Director, Office of Science, Office of Basic Energy Sciences, of the
40 U.S. Department of Energy under Contract No. DE–AC02–05CH11231. The authors thank the
41 editor, Linda M. (Prince) MacKechnie, and an anonymous reviewer for their constructive and
42 helpful comments.

43

44 ABSTRACT

- 45 • *Premise of the study:* Recent phylogenetic analyses based on molecular data suggested
46 that the monocot family Zingiberaceae be separated into four subfamilies and four tribes.
47 Robust morphological characters to support these clades are lacking. Seeds were
48 analyzed in a phylogenetic context to test independently the circumscription of clades and
49 to better understand evolution of seed characters within Zingiberaceae.
- 50 • *Methods:* Seventy-five seeds from three of the four subfamilies were analyzed using
51 synchrotron based X-ray tomographic microscopy (SRXTM) and scored for 39
52 morphoanatomical characters.
- 53 • *Key results:* Zingiberaceae seeds are some of the most structurally complex seeds in
54 angiosperms. No single seed character was found to distinguish each subfamily, but
55 combinations of characters were found to differentiate between the subfamilies.
56 Recognition of the tribes based on seeds was possible for Globbeae, but not for Alpinieae,
57 Riedelieae, or Zingibereae, due to considerable variation.
- 58 • *Conclusions:* SRXTM is an excellent, non-destructive tool to capture morphoanatomical
59 variation of seeds and allows for the study of taxa with limited material available.
60 Alpinioideae, Siphonochiloideae, Tamijioideae, and Zingiberoideae are well-supported
61 based on both molecular and morphological data, including multiple seed characters.
62 Globbeae are well-supported as a distinctive tribe within the Zingiberoideae, but no other
63 tribe could be differentiated using seeds due to considerable homoplasy when compared
64 to currently accepted relationships based on molecular data. Novel seed characters
65 suggest tribal affinities for two currently unplaced Zingiberaceae taxa: *Siliquamomum*

ACCEPTED MANUSCRIPT -----Benedict et al. Zingiberaceae Seed Morphoanatomy
66 may be related to Riedelieae and *Monolophus* to Zingibereae, but further work is needed

67 before formal revision of the family.

68 Keywords: aril; chalaza; embryo; ginger; micropyle; monocotyledon; operculum; seed coat;
69 synchrotron based X-ray tomographic microscopy (SRXTM); testa.

70

INTRODUCTION

71

72 Seeds are an integral part of a plant, but detailed information about them and their utility in
73 phylogenetic studies is limited. In a seminal work on dicotyledonous seed anatomy, Corner
74 (1976:vii) stated, "...classification without seed-structure is unsound and, consequently, our
75 knowledge of the evolution of flowering plants." Along with potentially clarifying systematic
76 relationships between taxa, data on seed morphoanatomy are also fundamental to addressing the
77 carpological fossil record, which in turn enlightens our understanding of evolution, paleoecology,
78 paleobiogeography, and past climate change (e.g., Manchester and Kress, 1993; Collinson and
79 van Bergen, 2004; Chen and Manchester, 2007; Collinson et al., 2012; Herrera et al., 2014).
80 Understanding seed structure also enhances our understanding of biological features that may
81 facilitate dispersal, inhibit or facilitate dormancy, and survivability – information particularly
82 relevant to germplasm banks, which strive to preserve biodiversity (e.g., Boesewinkle and
83 Bouman, 1995; Baskin and Baskin, 2001; Wada et al., 2011), and contribute considerably to the
84 proper identification of commercially important or potentially important plants (e.g., Vaughan,
85 1970; Wu et al., 2014) and food security. Thus, seed anatomical studies are important in a variety
86 of ways.

87 Zingiberaceae are an economically and ecologically important family of commelinid
88 monocots with a center of diversity in Southeast Asia (Kress et al., 2002; Larsen, 2005). It is the
89 largest and most species-rich family within Zingiberales and currently contains 52 genera and
90 approximately 1600 species, with an average of 13 new taxa being described a year for the past
91 two decades (The Plant List, 2013). Seeds of Zingiberales have been studied for more than a
92 century (Tschirch, 1891; Humphrey, 1896; Netolitzky, 1926; Mauriszon, 1936; Takhtajan, 1985).

93 More recently they have been studied in search of potential pharmacognostical characteristics
94 (see Liao and Wu, 1996 for a review), but little information is available on utilizing seeds as a
95 source of data for systematics and often these studies are limited in scope to a few species or
96 genera (Kimura and Yoshimura, 1968; Liao and Wu, 1996; Wu et al., 2014). Furthermore, many
97 early studies were the subject of inter-familial comparisons based often on immature seeds,
98 which do not demonstrate anatomical differences seen in later stages of development (e.g.,
99 Humphrey, 1896; see Takhtajan, 1985 for comparisons). One potential reason for the paucity of
100 studies on zingiberalean seeds is the presence of a hard, brittle seed coat with phytoliths, making
101 traditional paraffin embedding and microtomy difficult (Benedict, 2012; Benedict et al., 2015).
102 The use of synchrotron based X-ray tomographic microscopy (SRXTM) to analyze the seeds
103 provides high-resolution detail of seed coats and seed and embryo internal morphoanatomy. In
104 addition, SRXTM is non-destructive and requires no specimen-altering preparations (e.g., critical
105 point drying, rehydration, coating, etc.), which provides the opportunity to analyze rare material
106 from herbarium specimens and to standardize anatomical observations across a wide range of
107 taxa (Smith et al., 2009; Benedict et al., 2015).

108 Traditional circumscription of the Zingiberaceae by Schumann (1904), Holttum (1950),
109 Burt and Smith (1972), and Larsen et al. (1998) included four tribes (Alpinieae, Hedychieae,
110 Globbeae, and Zingibereae). Recent work, based on molecular data, recognizes four subfamilies
111 (Alpinioideae, Siphonochiloideae, Tamijioideae, Zingiberoideae) with tribe Zingibereae, tribe
112 Globbeae, and *Monolophus* (formerly *Caulokaempferia*; Mood et al., 2014) nested within
113 Zingiberoideae, and tribe Alpinieae, tribe Riedelieae, and *Siliquamomum* nested within
114 Alpinioideae (Table 1). Tamijioideae are monospecific and Siphonochiloideae contain two

115 genera (Kress et al., 2002; Table 1). All subfamilies are well-supported based on molecular and
116 morphological data, but many speciose genera (e.g., *Alpinia*, *Amomum*, and *Curcuma*) have been
117 shown to be paraphyletic and/or polyphyletic (*Amomum*: Harris et al., 2000, Xia et al., 2004;
118 *Alpinia*: Rangsiruji et al., 2000; Zingibereae: Ngamriabsakul et al., 2004; *Etilingera*: Pedersen,
119 2004; *Globba*: Williams et al., 2004; Alpinioideae: Kress et al., 2005, 2007; *Curcuma*: Závěská
120 et al., 2012; Leong-Škorníčková et al., 2015).

121 The family as a whole is easily separated from other Zingiberales families by possessing
122 ligulate distichous leaves, flowers with a single dithecal stamen, and an often showy petaloid
123 labellum formed from two or four staminodes (Simpson, 2010). Within Zingiberaceae, the plane
124 of distichy along a leafy shoot separates Alpinioideae (perpendicular to the rhizome) from the
125 other tribes (parallel to rhizome), but many other floral and vegetative characters previously used
126 to distinguish tribes (e.g., locule number, presence/absence of lateral staminodes) are not unique
127 to any particular subfamily or tribe (Kress et al., 2002). A single synapomorphic character was
128 suggested to distinguish Riedelieae from Alpinieae: the presence of extrafloral nectaries
129 approximately 2.5 cm above the petiole on the midrib or costa of the adaxial surface of the leaf
130 (Kress et al., 2002). This character has indeed been documented for all members of Riedelieae
131 (Mood, 1996; Larsen and Mood, 1998; Kress et al., 2002), but it has also been observed in
132 various species of Alpinioideae, e.g., *Amomum citrinum* (Ridl.) Holttum, *Amomum*
133 *xanthophlebium* Baker, *Hornstedtia sanhan* M.F.Newman, as well in Zingiberoideae, e.g.,
134 *Zingiber singaporense* Škorníčková. (Škorníčková, pers. obs.) and therefore cannot be used to define
135 Riedelieae. Unfortunately morphological characters useful for distinguishing various clades in

136 Zingiberaceae are exceeding rare, but are crucial for independently testing phylogenetic
137 hypotheses based on molecular data.

138 To date, a single preliminary systematic treatment of Zingiberaceae seeds by Liao and Wu
139 (2000) showed that the two main subfamilies can be distinguished based on anatomical details of
140 the endotesta, which is sclerenchymatous in Alpinioideae and parenchymatous with often
141 rectangular cells in Zingiberoideae. While this preliminary study was useful in documenting this
142 distinguishing character between the two subfamilies, it only documented four characters for the
143 60 taxa analyzed. This is true for many previous studies on Zingiberales seeds where very few
144 seed characters are incorporated into analyses, which limits their application in plant systematics
145 (e.g., three seed characters analyzed and discussed in Grootjen and Bouman, 1981; four seed
146 characters used in ordinal phylogenetic analyses in Kress, 1990; Kress et al., 2001).

147 A more recent study on seeds within subfamily Alpinioideae (Benedict et al., 2015)
148 showed that Zingiberaceae seeds are structurally some of the most complicated seeds in
149 angiosperms and documented 23 seed characters for the subfamily, many of which have not been
150 used to categorize seeds prior. Benedict et al. (2015) found that Riedelieae and Alpinieae can be
151 further distinguished based on endotesta structure and operculum layering, and that many of the
152 proposed clades of *Alpinia* sensu Kress et al. (2005, 2007) are supported by seed characters.
153 While these studies demonstrate the usefulness of seed characters in the systematics of
154 Alpinioideae, their utility for Zingiberaceae as a whole remains to be tested. It is the aim of this
155 paper to: 1) document novel characters not commonly described for Zingiberaceae seeds that
156 may prove useful for future studies on angiosperm systematic and seed ecology studies within
157 and outside of the Zingiberaceae, 2) provide details of seed morphology and anatomy of many

158 Zingiberaceae that have not been documented previously, 3) determine whether synapomorphic
159 characters exist for subfamilies and tribes within Zingiberaceae, and 4) determine if seed
160 characters can help resolve the correct placement of incertae sedis taxa within Zingiberaceae
161 sensu Kress et al. (2002, 2005, 2007).

162

163

MATERIALS AND METHODS

164 Mature dried seeds of seventy-five taxa from three of the four subfamilies of Zingiberaceae
165 were sampled from various herbaria, botanical gardens, or commercial growers (Table 2). The
166 number of seeds studied per taxon ranged from one to more than 50. Each species was examined
167 with light microscopy for external features and analyzed using synchrotron based X-ray
168 tomographic microscopy (SRXTM; also referred to in some literature as synchrotron radiation
169 X-ray computed tomography, SRXCT, or SR μ CT).

Light microscopy and photography—

171 External features of the seeds were observed using a Leica MZ6 (Leica Microsystems Inc.,
172 Illinois, USA) or Nikon SMZ1500 (Nikon Instruments Inc., New York, USA) stereomicroscope
173 and photographed using a Macropod (Macroscopic Solutions LLC, Coventry, CT, USA),
174 outfitted with a Canon EOS 6D DSLR with a Macro Photo MP-E 65mm manual focus lens, MT-
175 24EX Macro Twin Light flash, and a STKS-C StackShot Macro Rail (Cognisys Inc., Michigan,
176 USA). Series of 20–75 images at various focal planes were obtained and stitched into a single
177 image using Zerene Stacker version 1.04 software (Zerene Systems LLC, Washington, USA).
178 Images were edited uniformly for contrast using Adobe Photoshop CS2 (Adobe Systems Inc.,
179 California, USA).

180 *Synchrotron based X-ray tomographic microscopy—*

181 Samples were mounted onto brass stubs or toothpicks using a PVA glue or epoxy and
182 imaged using standard absorption contrast at the TOMCAT beamline at the Swiss Light Source
183 (SLS; Stampanoni et al., 2006; Paul Scherrer Institut, Villigen, Switzerland; specimens scanned
184 in 2009, 2010, 2011, 2013, and 2015); the 2-BM beamline at the Advanced Photon Source (APS;
185 Argonne National Laboratory, Lemont, IL; specimens scanned during sessions in 2011 and
186 2012); or the 8.3.2 beamline at the Advanced Light Source (ALS; MacDowell et al., 2012;
187 Lawrence Berkeley National Laboratory, Berkeley, California; specimens scanned during
188 session in 2013, 2014, and 2015). Transmitted X-rays were converted into visible light using a
189 20 μm (SLS: 2013, 2015), 100 μm (SLS: 2013, 2015; APS), or 200 μm scintillator (SLS: 2009–
190 2011) LAG:Ce scintillator screen (Crytur, Turnov, Czech Republic) or a 0.5 mm LuAG
191 scintillator (Crytur, Turnov, Czech Republic; ALS).

192 At TOMCAT, projection data were magnified by 2 \times , 4 \times , or 20 \times microscope objectives and
193 digitized by a high-resolution CCD camera (pco.2000; PCO GmbH, Kelheim, Germany; 2009–
194 2011) or sCMOS camera (pco.edge 5.5; PCO GmbH, Kelheim, Germany; 2013). Samples were
195 scanned using 10 or 13 keV and an exposure time per projection of 50, 125, 150 or 200
196 milliseconds. For each scan, a total of 1501 projections (2048 \times 2048 pixels with PCO.2000
197 camera, 2560 \times 2160 pixels with PCO.edge 5.5 camera) were acquired over 180°. Reconstruction
198 of the tomographic data was performed on a 60-node Linux PC cluster using a highly optimized
199 routine based on the Fourier transform method and a gridding procedure (Marone et al., 2010;
200 Marone and Stampanoni, 2012), resulting in a theoretical pixel size of 3.7 μm at 2 \times and 1.85 μm
201 at 4 \times (2009–2011) or 3.25 μm at 2 \times and 1.625 μm at 4 \times (2013–2015) for reconstructed images.

202 At 2-BM, 2.5×, 4×, or 5× microscope objectives were used to magnify the projection data,
203 and a Coolsnap K4 camera (Photometrics, Tucson, Arizona, 2011 and February 2012) or
204 pco.dimax high-speed camera (PCO GmbH, Kelheim, Germany, June 2012) was used to digitize
205 the data. Samples were scanned at 16.1 or 21 keV with an exposure time of 280–700 ms. For
206 each scan, a total of 1500 projections (2048×2048 pixels with Coolsnap K4, 2016×2016 for
207 PCO) were acquired over 180°. The tomographic reconstructions were conducted with a 64-node
208 cluster at APS using a gridrec reconstruction algorithm (Dowd et al., 1999). Reconstructed
209 images taken with the Coolsnap K4 had a theoretical pixel size of 3.7 µm at 2×, 2.96 µm at 2.5×,
210 1.85 µm at 4×, and 1.48 µm at 5×, and those taken with the pco.dimax had a theoretical pixel
211 size of 5.5 µm at 2×, 4.4 µm at 2.5×, 2.75 µm at 4x×, and 2.2 µm at 5×.

212 At the 8.3.2 beamline, samples were magnified with either a 2× or 5× microscope objective
213 and digitized using a sCMOS camera (pco.edge; PCO GmbH, Kelheim, Germany). Samples
214 were scanned at 15 keV with an exposure time of 90, 500, or 950 ms. For each scan, a total of
215 2049 projections (2560×2160 pixels) were acquired over 180°. Reconstruction was carried out
216 using a custom ImageJ (Rasband, 1997–2014) plugin for image preprocessing and Octopus
217 (Inside Matters, Aalst, Belgium) for tomographic reconstruction. Reconstructed images had a
218 theoretical pixel size of 3.25 µm at 2× and 1.3 µm at 5×.

219 Reconstructed images were processed at the University of Michigan using Avizo 7.0 or 8.0
220 (FEI Visualization Science Group, Burlington, Massachusetts, USA) for Windows 7. Images
221 were captured in Avizo 7.0 or 8.0 and edited uniformly for contrast using Adobe Photoshop CS2
222 or CS6 (Adobe Systems Incorporated, San Jose, California, USA).

223 *Character evolution analyses—*

224 Character states that were not observable due to scanning conditions or missing data were
225 treated as (?), and character states that were not applicable (e.g., character 14, operculum
226 layering if no operculum was present, character 13) were treated as (–) to distinguish a lost
227 character from a missing character in the character evolution analyses. The character matrix
228 (Table 3) was imported into Mesquite v.3.03 (Maddison and Maddison, 2015) and characters
229 were traced using parsimony onto a tree topology derived primarily from the results of the most
230 recent family level study by Kress et al. (2002), which used a combined nuclear internal
231 transcribed spacer (ITS) and plastid *trnK/matK* dataset. The Alpinioideae portion of the
232 phylogeny follows that of Kress et al. (2007), based on a combined ITS/*matK* dataset, because it
233 provided better resolution to the relationships of taxa within the subfamily. The placement of
234 *Newmania* as sister to *Haniffia* was taken from Leong–Škorničková et al. (2011), based on a
235 combined *trnK/matK* and ITS dataset as well, where the genus was first described and placed
236 into a phylogenetic context within the family. The *Hedychium* clade topology was derived from
237 Wood et al. (2000), which was based on an ITS1, ITS2, and 5.8S nuclear ribosomal DNA dataset.

238 RESULTS

239 All seeds were mature, dry, and possessed seed coats derived from outer integument (testa)
240 only; often comprising exotesta, mesotesta, and endotesta (Grootjen and Bouman, 1981;
241 Benedict et al., 2015). Seeds were analyzed for 39 internal and external seed characters (Table 3),
242 expanded and modified from the 23 characters identified by Benedict et al. (2015), to address the
243 large amount of variation in Zingiberaceae seeds. Characters were determined from observations
244 of seed external morphology and internal anatomy available from digital longitudinal and
245 transverse sections, 3-dimensional (3D) volume renderings, and movies of serial digital

246 longitudinal and transverse sections (between 1000–2000 sections per series). Some of the
247 characters introduced below may be correlated, but future developmental studies are needed to
248 determine if these correlations are developmental in nature. Digital sections and hand-colored
249 images of digital sections of selected taxa are provided to illustrate selected seed structures
250 discussed below (Figs. 1A–P).

251 ***Variation in Seed Structure—***

252 1. *Natural seed color*— Zingiberaceae seeds, when mature and dry, are often tan, red, or
253 light brown (e.g., Figs. 2A, 2F, 2K, 2P), but can also be dark brown to black (e.g., Figs. 4A, 7F)
254 or even white (Fig. 3A). Character states are scored as follows: 0, white; 1, tan/ red/ light brown;
255 2, dark brown/ black.

256 2. *Seed surface*— The surfaces of Zingiberaceae seeds can be striate (e.g., Figs. 6G, 7A,
257 9F), or verrucose (surfaces with small bumps, e.g., Fig. 8F). Character states are scored as
258 follows: 0, striate; 1, verrucose.

259 3. *Trichomes*— Trichomes may (Figs. 2E, 2J, 2O, 2T, 5E, at arrows) or may not be present
260 on the surface of the seed coat or aril. Character states are scored as follows: 0, absent; 1, present.

261 4. *Aril*— Arils and various fleshy, tubular, or disk-like appendages at the micropylar region
262 of the seed have been given various names based on the particular region of the seed or funiculus
263 from which they derive (Kapil et al., 1980). A detailed history and alternate classification is
264 given by Kapil et al. (1980), in which they propose — in agreement with Corner (1976) — that
265 all aril-like structures be called arils and terms such as arilloid, arillode, false aril, hilar aril, etc.,
266 be abandoned. They also propose that funicular arils, caruncles (derived from the exotesta, also
267 called an exostome-aril), and strophioles (derived from the raphe tissue) be retained for

268 descriptive purposes only. We adopt this interpretation of the definition of an aril, and choose to
269 describe arils in terms of presence and absence without making a distinction of exact origin
270 (integumentary, funicular, or raphe tissue) due to the limited developmental understanding of
271 many taxa within the family. While the origin of the aril is not always clear, the extent of the aril
272 may be useful in distinguishing between taxa. Arils may be solid structures confined to the
273 micropylar end of the seed (e.g., Figs. 2F, 7F, 7K, 9A), may consist of many separate strands
274 (e.g., Figs. 3F, 3K, 4P) or a few thick lobes (Fig. 8A) at the micropylar end; or may envelope
275 more than half of a seed and be tightly adpressed (e.g., Figs. 6A, 6E, 6J, 6O) or not (Figs. 3P–Q)
276 to the seed coat. Character states are scored as follows: 0, enveloping more than half of seed and
277 tightly adpressed to the seed coat; 1, present only at micropylar end of seed, solid structure; 2,
278 present only at micropylar end of seed, divided into many separate strands; 3, present only at
279 micropylar end of seed, divided into few thick lobes; 4, present, enveloping more than half of the
280 seed, but not tightly adpressed to the seed coat.

281 5. *and 6. Seed shape*— Seeds in Zingiberaceae (and indeed across Zingiberales) vary
282 considerably in their shape due, in part, to frequently tight packing within the fruit (Benedict and
283 Smith, pers. obs.; e.g., Figs. 2K, 7F). Therefore, seed shape was documented for those seeds
284 located closest to the middle of each fruit, showing the least compression.

285 5. *General seed shape*— Character states are scored as follows: 0, ellipsoid; 1, ovoid; 2,
286 oblate (flattened at the poles of the seed); 3, polyhedral.

287 6. *Seed contorted from arrangement in fruit*— Character states are scored as follows: 0, no
288 contortion of seeds from tight packing in fruit; 1, seed shape contorted by tight packing in fruit.

289 7. *Seed length*— Seed length also varies with respect to location within the fruit and a
290 binary character of “at least twice as long as wide” or “less than twice as long as wide” was used
291 to generalize seed length. Character states are scored as follows: 0, less than twice as long as
292 wide; 1, at least twice as long as wide.

293 8. *Seed body taper at micropylar region*— Character states are scored as follows: 0, absent;
294 1, present.

295 9. *Seed body taper at chalazal region*— In some seeds, the body has a slight decrease in
296 width, or taper, towards the chalazal region. Character states are scored as follows: 0, absent; 1,
297 present.

298 10. *Externally visible raphe*— During maturation of the seed, the anatropous ovules of
299 Zingiberaceae taxa may produce an externally visible groove or ridge in the seed coat
300 corresponding to the position of the raphe in the mature seed (Figs. 8A, 9A). Character states are
301 scored as follows: 0, absent; 1, present.

302 11. *External chalazal indentation*— As with the externally visible raphe (10), in some
303 Zingiberaceae the chalazal region of the seed has a distinctive circular indentation, termed a
304 "sunken chalaza" in *Costus* (Grootjen and Bouman, 1981). It is unclear if this structure is
305 homologous for Zingiberaceae seeds and future developmental work is needed to understand the
306 evolution of this trait across the order. Character states are scored as follows: 0, absent; 1,
307 present

308 12. *Micropylar region shape*— In longitudinal section, the micropylar region, sometimes
309 including a hilar rim, operculum, and micropylar mesotestal proliferation of cells, can range from
310 being conical (e.g., Figs. 1A–B, 1E–H, 4B, 4G), cylindrical (e.g., Figs. 1C–D, 3B, 3R), or not

311 clearly defined or absent. Character states are scored as follows: 0, absent/not clearly defined; 1,
312 conical; 2, cylindrical.

313 *13. Operculum*— An operculum is found within many Zingiberaceae and is conical to disk-
314 shaped in longitudinal section. Character states are scored as follows: 0, absent; 1, present.

315 *14. Operculum layering*— The operculum is derived from mesotesta and/or endotesta,
316 making them either homogeneous, or formed of two (or more) distinctive layers. In SRXTM
317 images, the inner, endotesta-derived layer often has an outer X-ray bright layer that forms a
318 boundary with the outer mesotestal-derived layer; this varies from being extremely thin (Figs.
319 1C–D) to more substantial (Figs. 1I–J). An outer layer from mesotesta tends to be formed of
320 larger cells, sometimes with intercellular spaces, and lacks the X-ray bright nature in SRXTM
321 images (Figs. 1G–H, 1K–L). Character states are scored as follows: (–) no operculum present; 0,
322 more or less homogeneous; 1, multilayered.

323 *15. Micropylar collar*— The micropylar collar (labelled “mc” in figures) is a tube or
324 cylinder of testal cells (see character 16) that expands into the embryo chamber, often creating
325 two ‘v’ shapes below the operculum in longitudinal section (Figs. 1C–F, 1I–L). Some seeds
326 appear to have shallowly or deeply infolded micropylar collars, but this character was found to
327 be subjective in nature and thus was not included as a separate character. The apical portion of
328 the micropylar collar is the attachment point for the operculum of many Zingiberaceae seeds and
329 often surrounds the apical portion of the embryo (e.g., Figs. 4L, 4Q, 8D). Character states are
330 scored as follows: 0, absent; 1, present.

331 *16. Micropylar collar layering*— The micropylar collar is formed either from the endotesta
332 or a combination of the endotesta and mesotesta. Liao and Wu (1996) recognized three types of

333 micropylar collars based on large-volume mesotestal cells (“form A”), small-volume mesotestal
334 cells (“form B”) or no mesotestal cells (“form C”). In our studies, the distinction of large and
335 small mesotestal cells was found to be based on subtle differences; therefore two are recognized
336 here, those that are formed from mesotesta and endotesta (=forms A or B; e.g., Figs. 1C–F, 1K–
337 L, 4L, 4Q, 7G, 7L) and those that are formed from endotesta only (=form C; e.g., 1I–J, 6K, 6P,
338 7B). Character states are scored as follows: (–), no micropylar collar present therefore character
339 not applicable; 0, formed from endotesta only; 1, formed from endotesta and additional layers.

340 *17. Thickened micropylar collar*— The micropylar collar sometimes shows a distinctly
341 thickened mesotesta in longitudinal section with respect to the rest of the seed coat (e.g., Figs.
342 1K–L, 4L, 7G, 7L). Character states are scored as follows: (–) no micropylar collar present
343 therefore character not applicable; 0, absent; 1, present.

344 *18. Recurved micropylar collar*— The inner terminus of the micropylar collar ranges from
345 being distinctly acute (strongly recurved, e.g., Figs. 1C–F, 7Q, 8D) to weakly recurved (e.g., Figs.
346 1K–L, 7G), in longitudinal section. Character states are scored as follows: (–) no micropylar
347 collar present therefore character not applicable; 0, weakly recurved; 1, strongly recurved.

348 *19. Hilar rim*— A hilar rim (labelled “hr” in figures) is an elongated tube of seed coat that
349 forms a rim at the micropylar region of the seed. In longitudinal section it was previously
350 described as “[it] produces the appearance of a pair of horns arising from the hilar end of the
351 seed” (Manchester and Kress, 1993:1267; e.g., Figs. 1C–D, 2B, 2G, 3B, 7B, 8D, 10A–B). In
352 some specimens the rim recurves slightly inwards, especially when the aril has been detached
353 (e.g., Figs. 2G, 3B). Character states are scored as follows: 0, absent; 1, present.

354 20. *Hilar rim layering*— The hilar rim can be formed from the exotesta (e.g., Fig. 7B) or a
355 combination of the exotesta and mesotesta (e.g., Figs. 1C–D, 3B, 4B, 5G). Character states are
356 scored as follows: (–) no hilar rim present therefore character not applicable; 0, formed from
357 exotesta; 1, formed from exotesta and mesotesta.

358 21. *Micropylar mesotestal proliferation*— The mesotesta of the micropylar region of the
359 seed may have a proliferation of cells to produce a mass of cells in the shape of a donut or
360 cylinder (labelled “mmp” in figures). In longitudinal section this proliferation of cells is adjacent
361 to the operculum, above and offset from the micropylar collar (e.g., Figs. 1C–D, 5L, 7B).
362 Character states are scored as follows: 0, absent; 1, present, bulbous and wide (donut shaped; e.g.,
363 Figs. 5L, 6B); 2, present, cylindrical and narrow (e.g., 3B).

364 22–24. *Chalazal modifications*— Chalazal modifications of Zingiberaceae seeds are
365 divided into two general forms: testal proliferations (masses of mesotestal cells that have
366 undergone extra periclinal divisions in the chalazal region compared to the rest of the seed coat
367 and contribute three or more rows of cells to the seed coat; characters 22 and 23) and chalazal
368 chambers (empty cavities nested within the mesotesta of seed coats; character 24). Testal
369 proliferations do not include raphe and chalazal pigment group cells. Two types of testal
370 proliferations exist: i) a simple mass of mesotestal cells (e.g., Figs. 1O–P, 2M, 2R, 3C, 3M, 7H;
371 labeled “cmp” in figures), here termed massive, and ii) a wall or column of endotestal and
372 mesotestal cells that vertically divides the lower portion of the embryo cavity into two segments,
373 termed here a columnar mesotestal proliferation (Figs. 1M–N). These two chalazal modifications
374 are not mutually exclusive and taxa can have both a chalazal chamber and a proliferation of
375 mesotestal cells.

376 22. *Massive chalazal testal proliferations*— Character states are scored as follows: 0,
377 absent; 1, present.

378 23. *Columnar chalazal testal proliferations*— Character states are scored as follows: 0,
379 absent; 1, present.

380 24. *Chalazal chamber*— Two distinct types of chalazal chambers (labelled “cc” in figures)
381 have been identified in Zingiberaceae seeds, the *Alpinia*-type and the *Amomum*-type. The
382 *Alpinia*-type is typically lens-shaped and less than 1/3 the width of the seed (e.g., Figs. 1M–N,
383 5H, 9E) whereas the *Amomum*-type is more than 1/3 the width of the seed and often connects to
384 (and becomes continuous with) the raphe canal in the seed (e.g., Figs. 3C, 6B, 6F). Character
385 states are scored as follows: 0, absent; 1, *Alpinia*-type; 2, *Amomum*-type.

386 25. *Chalazal mucro*— A chalazal mucro (labelled “cm” in figures) – an abrupt, pointed
387 termination of the seed (in contrast to character 9, which is a gradual tapering of the seed body) –
388 was reported by Ridley (1909) where he suggested the structure (termed “terminal mucro”) was a
389 modification for water and wind dispersal in *Burbridgea*. It has since also been found in other
390 Alpinioideae as well (Benedict et al., 2015). The structure is composed of endotesta, mesotesta,
391 and exotesta (Figs. 7A, 7C, 8E). Character states are scored as follows: 0, absent; 1, present.

392 26. *Seed coat thickness*— The seed coat (all layers of the testa) thickness is determined in
393 transverse sections in the middle of the seed and is measured at the thinnest region of the seed
394 coat. Character states are scored as follows: 0, 1–99 μm ; 1, 100–199 μm ; 2, ≥ 200 μm .

395 27. *Exotesta cell type*— The exotesta can be made of palisade cells (e.g., Figs. 7D, 7I),
396 generally isodiametric cells (e.g., Fig. 6H), be poorly developed (e.g., 3D), or it can be absent.

397 Character states are scored as follows: 0, palisade; 1, more or less isodiametric or cuboidal; 2,
398 poorly developed or destroyed in mature seed.

399 28. *Uniform exotesta*— The exotesta is most commonly composed of a homogeneous layer
400 of cells, but it can also be heterogeneous with cells that vary in shape as a result of irregular
401 anticlinal divisions of the exotesta (e.g., Figs. 2S, 3T). Character states are scored as follows: 0,
402 homogeneous; 1, heterogeneous.

403 29. *Multiseriate exotesta*— Previously described as a multiple epidermis by some authors
404 (e.g., Wu and Liao, 1995; Liao and Wu, 2000), the exotesta is often uniseriate, but can be
405 multiseriate with two or more cell layers (e.g., Fig. 2N). Character states are scored as follows: 0,
406 absent; 1, present.

407 30. *Number of types of mesotestal cells*— The mesotesta, when differentiated, is composed
408 of three cell types occurring in distinct layers in Zingiberaceae seeds (Liao and Wu, 1996, 2000).
409 These layers have been previously described as the hypodermis (directly beneath the exotesta),
410 the translucent cell layer (beneath the hypodermis) and the pigment layer (beneath the
411 translucent cell layer and above the endotesta). In some taxa, the three types can be discerned
412 (e.g., Fig. 4I), whereas in others it is either absent, a single type (e.g., Figs. 6D, 6H), or two types
413 (e.g., Figs. 4S, 9G). Character states are scored as follows: 0, absent; 1, one type; 2, two types; 3,
414 three types.

415 31. *Endotestal cell thickness and shape*— The endotesta is the innermost layer of cells of
416 the seed coat in Zingiberaceae seeds. Its thickness and shape vary considerably and can range
417 from very small square to rectangular sclerified cells that are less than 30 μm in thickness (e.g.,
418 Fig. 6N), to palisade sclerified cells 30 μm or greater in thickness (e.g., 6D, 6H), to a thin layer,

419 <15 μm , of parenchyma cells (e.g., Figs. 2N, 2S, 3T). Character states are scored as follows: 0,
420 thin parenchyma (<15 μm thickness); 1, short sclerenchyma (15–30 μm in thickness); 2, elongate
421 sclerenchyma (≥ 30 μm in thickness).

422 32. *Endotestal gap location*— The endotesta has a small circular to ellipsoid interruption,
423 often in the chalazal region of seed, and typically represents the point where the raphe terminates
424 in the seed coat. In longitudinal section, this endotestal gap is filled by the chalazal pigment
425 group so is not seen as a true void (e.g., Figs. 1M–P, 6L, 6Q). The location of the gap varies
426 from being at the base of the seed (Fig. 6Q) to the side of the seed (Fig. 7R). Character states are
427 scored as follows: 0, present at the chalazal end; 1, present on the side.

428 33. *Chalazal pigment group*— As noted in previous studies (Liao and Wu, 1996, 2000), the
429 chalazal pigment group (cpg) is a small collection of cells in the embryo cavity above the raphe
430 and endotestal gap. Previously it was determined that members of Zingiberoideae have a discoid-
431 shaped cpg, termed ‘crescent-shaped’ by Liao and Wu (2000; Figs. 1O–P, 5M), while members
432 of Alpinioideae have ‘trumpet-shaped’ cpgs (Liao and Wu, 2000) or otherwise non-discoid cpgs
433 (Figs. 1M–N, 6L). Character states are scored as follows: 0, discoid-shaped; 1, non-discoid-
434 shaped.

435 34. *Raphe canal*— The raphe in mature seeds is destroyed on some taxa, leaving a canal in
436 the seed coat from the micropyle to the chalaza (Fig. 6F; labeled “rc” in figures). In some
437 specimens the raphe canal terminates at (and merges with) the chalazal chamber (e.g., Fig. 6F),
438 but can be differentiated from the chalazal chamber by being slightly smaller in diameter.
439 Character states are scored as follows: 0, absent; 1, present.

440 35. *Embryo length*— The embryos in most Zingiberaceae are elongate and extend for more
441 than half the length of the seed, but in some taxa they are much shorter. Character states are
442 scored as follows: 0, elongate; 1, short.

443 36. *Embryo shape*— The shape of the embryo ranges from being straight (Fig. 8C), L-
444 shaped (with a sharp, nearly right-angled curve in the embryo that is less than 25% of the embryo
445 length, Fig. 9B), to J-shaped (with a smooth curve in the embryo that is ca. 50% of the embryo
446 length, Fig. 6F). Character states are scored as follows: 0, straight; 1, L-shaped; 2, J-shaped.

447 37. *Embryo base*— Independent of shape, some taxa have embryos that are enlarged
448 (bulbous; e.g., Figs. 3M, 5Q) or forked (e.g., Fig. 6B) at the base. Character states are scored as
449 follows: 0, not differentiated; 1, bulbous; 2, forked.

450 38. *Embryo–testa contact*— The embryo, perisperm, and sometimes endosperm occupy the
451 embryo cavity of Zingiberaceae seeds. The embryo can either be in direct contact with the seed
452 coat (Figs. 9E) or nested within endosperm/perisperm and not touching the innermost wall of the
453 seed coat. Character states are scored as follows: 0, absent; 1, present.

454 39. *Basally proliferated endosperm* — Endosperm in some taxa is found in greater
455 abundance surrounding the base of the embryo (e.g., Figs. 3S, 4M, 6F) compared to the
456 micropylar end. In some SRXTM images perisperm is often composed of large cells (e.g., Fig.
457 5C) and endosperm is often darker and lacks observable cell walls (e.g., Fig. 6F). In other
458 SRXTM images endosperm appears as small cells (perhaps nuclei; e.g., 5R) and individual
459 perisperm cells are indistinguishable (e.g., Fig. 5R). In both cases endosperm always
460 immediately surrounds the embryo and both the embryo and endosperm are nested within the
461 perisperm (e.g., 2R, 5C, 7H, 9C). This character refers to the relative distribution of endosperm,

462 and whether it is proliferated, or more abundant, toward the chalazal end of the seed as compared
463 to the micropylar end. Character states are scored as follows: 0, absent; 1, present, weak or
464 minimal amount; 2, present, strong or copious amount.

465 *Zingiberaceae seeds in a systematic context—*

466 Results for all species studied are summarized in Table 3. All tribes of Alpinioideae and
467 Zingiberoideae were sampled as well as the subfamily Siphonochiloideae, which was previously
468 unknown for seed morphoanatomy. It was not possible to study the monospecific subfamily
469 Tamijioideae as no herbarium we contacted (E, K, MO, MICH, NY, SING, US) had fruit or seed
470 material available.

471 *Zingiberoideae—* Fourteen genera and 26 species representing both tribes were examined
472 (Figs. 1A–F, 1O–P, 2A–T, 3A–U, 4A–T, 5A–T). The seeds of the 26 species studied from
473 Zingiberoideae have in common 10 character states (character numbers in parentheses). They all
474 lack an externally visible raphe (10), have no columnar chalazal testal proliferation of cells (23),
475 no chalazal mucro (25), and their embryos are nested within nutrient tissue and do not contact
476 the endotesta (38). All Zingiberoideae seeds have seed coats less than 100 μm in thickness (26;
477 Figs. 2D, 2I, 2N, 2S, 3D, 3I, 3N, 3T, 4D, 4I, 4N, 4S, 5D, 5I, 5N, 5S), a hilar rim formed from
478 exotestal and endotestal layers (19 and 20; Figs. 2B, 2G, 2L, 2Q, 3B, 3G, 3L, 3R, 4B, 4G, 4L,
479 4Q, 5B, 5G, 5L), a thin endotesta of parenchyma (31; Figs. 2D, 2I, 2N, 2S, 3D, 3I, 3N, 3T, 4D,
480 4I, 4N, 4S, 5D, 5I, 5N, 5S), an endotestal gap at the base of the seed (32; e.g., Fig. 1O–P), and a
481 discoid chalazal pigment group (33; Figs. 1O–P, 5M).

482 The seven species of all three genera within Globbeae (Figs. 2A–T) have in common 16
483 characters. All seeds are lightly pigmented (tan, red, or light brown) (1; Figs. 2A, 2F, 2K, 2P),

484 have trichomes on either the surface of the seed or aril (3; Figs. 2E, 2J, 2O, 2T), an aril confined
485 to the micropylar end of the seed that is a solid structure (4; Figs. 2F, 2K, 2P), a hilar rim formed
486 from both the exotesta and mesotesta (19 and 20; Figs. 2B, 2G, 2L, 2Q), seed coats less than 100
487 μm thick (26; Figs. 2D, 2I, 2N, 2S), a thin parenchymatous endotesta (31; Figs. 2D, 2I, 2N, 2S),
488 an endotestal gap at the base of the seed (32), a discoid-shaped chalazal pigment group (33), and
489 elongate embryos that are not differentiated at the base and do not touch the endotesta (35, 37,
490 38; Figs. 1C, 1H, 1R). They all lack an externally visible raphe (10), a columnar chalazal testal
491 proliferation of cells (23), a chalazal mucro (25), and a uniform exotesta (28; 2D, 2I, 2N, 2S). A
492 micropylar collar (15) was found in all taxa except *Globba spathulata* Roxb. (Fig. 2Q). The
493 combination of a weakly recurved micropylar collar (19; Figs. 2B, 2G), the absence of basally
494 proliferated endosperm (39; Figs. 2C, 2H), and the presence of an external chalazal indentation
495 (11) were found to unite *Hemiorchis* sp. and *Gagnepainia harmandii* (Baill.) K.Schum. and
496 differentiate these two genera from *Globba*.

497 Ten genera and eighteen species were analyzed within the tribe Zingibereae (Figs. 3A–U,
498 4A–T, 5A–T) and found to have 13 characters in common. Seeds all have a hilar rim formed
499 from the exotesta and mesotesta (19 and 20; Figs. 3B, 3R, 4Q), seed coats less than 100 μm in
500 thickness (26; Figs. 3D, 3I, 3N, 3T, 4D, 4I, 4N, 4S, 5D, 5I, 5N, 5S), a thin parenchymatous
501 endotesta (31), an endotestal gap at the base of the seed (32; Figs. 1O–P, 5M), a discoid chalazal
502 pigment group (33; Fig. 5M), and an elongate embryo that does not contact the endotesta (35 and
503 38; Figs. 3M, 3S, 4H, 4M, 4R, 5M). They lack an externally visible raphe (10), columnar
504 chalazal testal proliferations (23), a chalazal mucro (25), and a uniform or multiseriate exotesta
505 (28 and 29). A bulbous embryo base (37) was found in *Newmania* (Fig. 3M) only, and a

506 micropylar collar (15) was found in all but two species, *Camptandra ovata* Ridl. (Fig. 5B) and
507 *Cautleya gracilis* (Sm.) Dandy (Fig. 4B). The shape of the seed (5) and the embryo (36), as well
508 as the type of cells in the exotesta (27), were all found to be quite variable in the tribe and not
509 useful in distinguishing the tribe from other Zingiberaceae.

510 The seeds of *Monolophus sikkimensis* (King ex Baker) Veldkamp & Mood are the smallest
511 described for Zingiberaceae (1.1 mm long × 0.6 mm wide) and can be distinguished from all
512 other Zingiberaceae by the absence of a micropylar collar (15; Fig. 5Q), presence of a short,
513 straight, bulbous embryo (35–37; Fig 5Q), and having basally proliferated endosperm that fills
514 more than half of the embryo cavity (39; Fig. 5R).

515 *Alpinioideae*— Sixteen genera and 46 species were examined from Alpinioideae (Figs.
516 6A–S, 7A–T, 8A–G), representing both tribes. Two characters are shared among all alpinoid
517 taxa: lack of a multiseriate exotesta (29; Figs. 6D, 6H, 6N, 6S, 7D, 7I, 7N, 7S, 8G), and the
518 presence of a non-discoid chalazal pigment group (33; e.g., Figs. 1M–N, 6L, 6Q, 7H).

519 Eleven genera and 40 species from the tribe Alpinieae (Figs. 6A–S) were analyzed. Seven
520 characters were found in common. All seeds of Alpinieae lack trichomes (3; Figs. 6C, 6G, 6M,
521 6R), have an operculum (13; Figs. 6B, 6F, 6I, 6K, 6P), have a micropylar collar (15; Figs. 6I, 6K,
522 6P), lack a chalazal mucro (25; Figs. 6A, 6E, 6J, 6O), and lack a multiseriate exotesta (29; Figs.
523 6D, 6H, 6N, 6S). Characters that were present in all Alpinieae studied were a non-discoid
524 chalazal pigment group (33; Figs. 1M–N, 6L, 6Q), and basally proliferated endosperm (39; Figs.
525 6F, 6Q). A hilar rim (19) was lacking in all Alpinieae except *Aframomum* species. *Alpinia boia*
526 Seem. was the only taxon observed to have an embryo in contact with the endotesta (38). Both

527 the presence and type of aril (4) and the shape of the embryo (36) were quite variable within the
528 tribe and not useful for distinguishing the tribe from other Zingiberaceae.

529 The five species of Riedelieae (Figs. 7A–T) that were analyzed had 12 seed characters in
530 common. All seeds of Riedelieae lacked an externally visible raphe (10), a columnar chalazal
531 chamber (23), a chalazal chamber (24), and a multiseriate exotesta (29). They all shared the
532 presence of an operculum (13; Figs. 7B, 7G, 7L, 7Q), the presence of a micropylar collar (15; 7B,
533 7G, 7L, 7Q), seed coats less than 100 μm thick (26; Figs. 7D, 7I, 7N, 7S), an exotesta of
534 isodiametric or cuboidal cells (27; Figs. 7D, 7I, 7N, 7S), a non-discoid chalazal pigment group
535 (33; Figs. 7H, 7R), an elongated embryo (35; Figs. 7M, 7R), an embryo that is not modified at
536 the base (37; Figs. 7H, 7M, 7R), and an embryo that does not touch the endotesta (38; Figs. 7H,
537 7M, 7R).

538 Many other characters were present in most, but not all, of the Riedelieae and thus are
539 potentially useful for narrower taxonomic groups but are not useful for identifying the tribe.
540 Generally the tribe had striate seeds (2), lacked trichomes (3), and had a uniform exotesta (28),
541 but in *Siamanthus siliquosus* K.Larsen & Mood verrucose seeds with trichomes (3) and a non-
542 uniform exotesta (28) were observed (Figs. 7A, 7S–T). In *Burbidgea stenantha* Ridl. (Figs. 7A–
543 E), elongate seeds (7), with a few-stranded aril (4), and chalazal mucro (25), were observed in
544 contrast to relatively short seeds, with a solid aril, and no chalazal mucro as seen in the other
545 members of Riedelieae. *Riedelia* sp. was found to have a homogeneous operculum (14), and a
546 single type of mesotestal cells (30), counter to the heterogeneous opercula and a mesotesta of
547 two distinct cell types observed in all other members of the tribe. The combination of a verrucose
548 seed surface (2), presence of trichomes (3), and a non-uniform exotesta (28) was unique to

549 *Siamanthus siliquosus* (Figs. 7P–T). A few stranded aril (4), elongate seed (7), and chalazal
550 mucro (25) in combination were found only in *Burbridgea stenantha*. The seed of
551 *Pleuranthodium* sp. (Figs. 7F–J) did not significantly taper at the chalaza (9), but had an external
552 chalazal indentation (11) and a chalazal proliferation of cells (22) resulting in a suite of character
553 states that differed from all other Riedelieae studied.

554 The large and elongate seeds of *Siliquamomum tonkinense* Baill. (Figs. 8A–G) can be
555 easily distinguished from other Zingiberaceae by the presence of an aril confined to the
556 micropylar region of the seed that is separated into two or three thick strands (4; Fig. 8A),
557 conspicuous trichomes on the aril and seed coat (3; Figs. 8A, 8F), a single externally visible
558 raphe (10; Fig. 8B), and a distinctive chalazal mucro at the base of the seed (25; Figs. 8C, 8E).

559 Finally, three characters in particular were found to have considerable variation within the
560 Riedelieae: the overall shape of the seed (5), and the thickness (17), and recurvature (18) of the
561 micropylar collar.

562 *Siphonochiloideae*— Two genera and three species were analyzed for Siphonochiloideae
563 (Figs. 9A–G). They can be distinguished from all other Zingiberaceae by a combination of
564 characters that includes a solid aril confined to the micropyle of the seed (4; Fig. 9A, 9D), the
565 absence of a micropylar collar (15; Fig. 9D), and the presence of a distinct externally visible
566 raphe from the micropyle to the chalaza of the seed (10; Fig. 9A).

567

568

DISCUSSION

569 The complexity of key aspects of the Zingiberaceae seeds (notably in micropylar, hilar and
570 chalazal regions; but also in presence of both perisperm and endosperm and variation in embryo

571 shape and testa) enables recognition of multiple characters and character states not available in
572 plant groups with simpler seed organization. In addition, the use of non-destructive SRXTM
573 substantially increases confidence in the assessment of characters because artifacts of physical
574 sectioning (such as tears within tissues caused by sectioning, spaces linked to shrinkage during
575 embedding, and distortion linked to different tissue response to sectioning or embedding media)
576 are all avoided (a point emphasized by Smith et al., 2009). The only artifacts that need to be
577 taken into account are those of shrinkage and distortion during seed drying naturally or for
578 herbarium preparation, which were accounted for as all scanned seeds were dry prior to scanning.
579 Furthermore, the ability to examine multiple planes of section in SRXTM datasets reinforces
580 character state documentation. Thus, in combination, seed complexity and observation by
581 SRXTM provide a powerful tool for phylogenetic analyses by yielding multiple characters and
582 character states that can be applied in evaluating relationships within Zingiberaceae.

583 While no single seed character state was found to be unique to any single subfamily,
584 combinations of seed character states were found that can be used to distinguish between the
585 three subfamilies Alpinioideae [absence of a multiseriate exotesta (29), short to elongate
586 sclerified endotesta (31), and a non-discoid chalazal pigment group (33)], Siphonochiloideae [a
587 solid aril (4), an externally visible raphe (10), and lack of a micropylar collar (15)], and
588 Zingiberoideae [lack of an externally visible raphe (10), a hilar rim of exotesta and mesotesta (19
589 and 20), no columnar chalazal proliferations (23), no chalazal mucro (25), seed coat 100–199 μm
590 in thickness (26), an endotesta of thin parenchyma (31), an endotestal gap at the base of the seed
591 (32), a discoid chalazal pigment group (33), and embryos that do not contact the testa (38)]
592 (Table 3; Fig. 10A–B). In contrast, at the tribal level, the only tribe with a unique combination of

593 character states not possessed by any other taxon outside of the tribe was Globbeae; Alpinieae,
594 Riedelieae, and Zingibereae were found to have distinctive characters to support the tribes, but
595 these characters or character states were also occasionally found in taxa outside the tribe.

596 Of the 39 characters analyzed, 22 were found to be informative for distinguishing the
597 subfamilies and tribes as currently recognized, whereas 17 were found to be variable at both the
598 subfamily and tribal level and are not useful for distinguishing tribes or subfamilies (Table 3).

599 The informative characters that allowed for differentiation of the tribes and subfamilies are: seed
600 color (1), trichomes on seed coat or aril (3), aril type (4), an externally visible raphe (10), an
601 external chalazal indentation (11), an operculum (13), a micropylar collar (15), a hilar rim (19),
602 the layering of the hilar rim (20), a columnar chalazal testal proliferation (23), a chalazal
603 chamber (24), a chalazal mucro (25), the thickness of the testa (26), a uniform exotesta (28), a
604 multiseriate exotesta (29), the shape of the endotestal cells (31), the location of an endotestal gap
605 (32), a chalazal pigment group (33), the length of the embryo (35), differentiation of the embryo
606 base (37), contact of the embryo with the endotesta (38), and basally proliferated endosperm (39).
607 Uninformative characters that were either too variable within a group or commonly found among
608 different groups are: the surface of the seed (2), the shape of the seed (5), seed contortion (6),
609 seed length (7), tapering of the seed body at the micropyle (8), tapering of the seed at the chalaza
610 (9), the shape of the micropylar region (12), the layering of the operculum (14), the layering of
611 the micropylar collar (16), a thickened micropylar collar (17), a recurved micropylar collar (18),
612 a micropylar mesotesta proliferation of cells (21), massive chalazal testal proliferations (22), the
613 type of exotestal cells (27), the number of types of mesotestal cells (30), the raphe canal (34),
614 and the shape of the embryo (36).

615 *Siphonochiloideae*—

616 The two genera of Siphonochiloideae shared a mosaic of character states with members of
617 Alpinioideae and Zingiberoideae, which is not surprising as they are sister to the rest of the
618 Zingiberaceae (Kress et al., 2002; Fig. 10B). Some members of both Siphonochiloideae and
619 Alpinioideae have a distinctive externally visible raphe (10) and embryos that touch the
620 endotesta (38), two characters lacking in all Zingiberoideae. All members of Siphonochiloideae
621 analyzed and some Zingiberoideae have a parenchymatous endotesta (31), a discoid-shaped
622 chalazal pigment group (33), and are lacking any evidence of a micropylar collar (15), which is
623 in direct contrast to Alpinioideae, where not a single member lacks a micropylar collar (15) and
624 all members have a sclerenchymatous endotesta (31) and trumped-shaped chalazal pigment
625 group (33).

626 *Zingiberoideae*—

627 Zingiberoideae seeds show a unique combination of 10 character states (Table 3). Two of
628 these character states, an endotesta of parenchymatous cells (31) and a discoid-shaped chalazal
629 pigment group (33) have been previously used to unite the subfamily (Liao and Wu, 2000), and
630 are reported here for the first time in the previously unstudied genera *Boesenbergia*, *Camptandra*,
631 *Distichochlamys*, *Newmania*, *Gagnepainia*, and *Hemiorchis* (Liao and Wu, 2000). Interestingly,
632 the two aforementioned character states are also found within the earliest diverging lineage of
633 Zingiberaceae, Siphonochiloideae. The other ten character states, introduced here for the first
634 time, help reinforce the relationships of members of the Zingiberoideae.

635 The Globbeae were found to possess a unique combination of 16 character states in the
636 seven species analyzed, and a combination of three character states — a light colored seed (1),

637 the presence of trichomes (3), and an undifferentiated embryo base (37) — can be used to
638 distinguish the tribe from other Zingiberaceae. *Boesenbergia curtisii* (Baker) Schltr. was very
639 similar to Globbeae members, but differed in having a white seed (36), where all Globbeae seeds
640 are either red or tan and never white or black in color. *Newmania* and *Monolophus sikkimensis*
641 were also similar to Globbeae, but differed in having a bulbously differentiated embryo base, a
642 character not seen in Globbeae. It was reported previously that Zingibereae (then separated into
643 Hedychieae and Zingibereae) can be distinguished from Globbeae on the basis that *Globba*
644 *racemosa* Sm. has a multiseriate exotesta (Liao and Wu, 2000), but in our expanded sampling of
645 the tribe including all three genera, it was found that a multiseriate exotesta (29) is lacking in
646 *Globba spathulata*, *Gagnepainia harmandii*, and *Hemiorchis* sp., thus eliminating the utility of
647 this character to separate the Globbeae from the Zingibereae.

648 The Zingibereae share 13 character states in common for the 18 species analyzed (Table 3),
649 but these character states are not unique to Zingibereae, as *Globba spathulata* has an identical
650 combination of character states for the same 13 characters. The other members of Globbeae
651 differ from Zingibereae in either possessing an external chalazal indentation (*Hemiorchis* and
652 *Gagnepainia harmandii*) or a multiseriate exotesta (*Globba pendula*, *G. sessiliflora* Sims, *G.*
653 *aurea* Elmer, and *G. maculata* Blume).

654 *Alpinioideae*—

655 Seed morphoanatomy is extraordinarily diverse (see Benedict et al., 2015 for discussion),
656 but a combination of two character states unites the subfamily: a uniseriate exotesta (29), and a
657 non-discoïd chalazal pigment group (33). A non-discoïd chalazal pigment group (33) and
658 sclerenchymatous endotesta (31) were originally reported by Liao and Wu (2000) in five genera

659 (*Alpinia*, *Amomum*, *Etlingeria*, *Hornstedtia*, and *Plagiostachys*) and 43 species to unite the
660 subfamily and corroborated by Benedict et al. (2015) in a broader analysis of the subfamily that
661 included *Aframomum* spp., *Burbidgea stenantha*, *Geocharis aurantiaca* Ridl., *Geostachys*
662 *densiflora* Ridl., *Pleuranthodium* sp., *Renealmia* spp., *Siamanthus siliquosus*, *Siliquamomum*
663 *tonkinense*, and *Vanoverberghia sepulchrei* Merr. We have since sampled more Alpinioideae
664 (introduced here) including more species of *Alpinia*, *Aframomum*, and *Hornstedtia*, and
665 *Elettariopsis unifolia* (Gagnep.) M.F.Newman, and have found the characters mentioned above
666 to be consistent in all Alpinioideae examined. It is important to note that our endotesta character
667 (31) includes thickness, cell shape, and cell type, and is not directly equivalent to Liao and Wu's
668 (2000) character. It is consistent with respect to a sclerenchymatous or parenchymatous cell type,
669 however cells vary in thickness within the subfamily.

670 The Alpinieae share seven character states among the 40 species analyzed (Table 3), but
671 the combination of these character states is not unique to the tribe. *Pleuranthodium* (Riedelieae)
672 is identical with respect to these character states, while *Siamanthus siliquosus* (Riedelieae) is
673 similar to Alpinieae taxa but is easily distinguished by conspicuous trichomes (3) on the exotesta,
674 a character lacking in all Alpinieae. *Riedelia* spp. and *Burbidgea stenantha* (Riedelieae) are also
675 similar in morphoanatomy with Alpinieae, but lack a well-formed basally proliferated endosperm
676 (39).

677 Five species representing the four genera of Riedelieae were analyzed and are found to
678 share 12 character states. However, the combination of these characters is not unique to
679 Riedelieae, and is also found in *Vanoverberghia sepulchrei* (Alpinieae). It is notable that all

680 studied members of Riedelieae lack a chalazal chamber (24), which is often present in seeds of
681 Alpinieae.

682 ***Unplaced taxa: Siliquamomum tonkinense and Monolophus sikkimensis***—

683 In recent studies based on molecular data *Siliquamomum tonkinense* was placed as either
684 sister to the *Alpinia rafflesiana* clade, which was then sister to the remaining Alpinieae (Kress et
685 al., 2005) or in a polytomy with Riedelieae and the rest of Alpinieae (sensu Kress et al., 2007), or
686 with low bootstrap support (<50%) as the earliest diverging lineage sister to the rest of
687 Riedelieae (sensu Kress et al., 2002). When seed morphoanatomical character states of
688 *Siliquamomum tonkinense* were analyzed, one character state, an externally visible raphe (10),
689 was found in some members of Alpinieae, but not in any Riedelieae, and three character states
690 [the presence of trichomes (3), a chalazal mucro (25), and weak basally proliferated endosperm
691 (39)] were found to ally it with members of Riedelieae. Additionally, when *Siliquamomum*
692 *tonkinense* was compared to Alpinioideae taxa surveyed here, it was found to be most similar to
693 *Burbidgea stenantha*, sharing 31 of the 39 seed character states analyzed. In parsimony analyses,
694 both with and without added characters from DNA sequence data, *Siliquamomum tonkinense* is
695 shown to be closely related to *Burbidgea* and never sister to *Alpinia rafflesiana*, as suggested by
696 previous authors (data not shown). In fact, only 17 of the 39 seed characters are shared between
697 the latter two taxa, the lowest number of characters shared between any Alpinioideae and
698 *Siliquamomum tonkinense* (Table 3). Based on the available morphological and molecular data it
699 is most parsimonious to conclude that *Siliquamomum* be included as a member of Riedelieae, but
700 more morphological and molecular data are needed confirm its relationship with either tribe.

701 *Monolophus* is the only genus currently unplaced in the Zingiberoideae based on a
702 combined ITS and *matK* dataset (Kress et al., 2002). Larsen and Smith (1972) postulated a close
703 relationship with *Camptandra* and *Boesenbergia*, but that was not supported based on molecular
704 work and the genus remains unplaced (Kress et al., 2002). Seeds of *Monolophus sikkimensis*
705 were analyzed and compared to other Zingiberoideae, and found to have one character state
706 unique to Globbeae, a single type of mesotestal cells (30), and two character states indicative of
707 Zingibereae, a poorly developed exotesta (27) and a bulbous embryo (37). Although further
708 information is needed to make a formal placement of *Monolophus*, it may be more closely
709 related to Zingibereae based on our reported seed characters.

710 ***Notable character state changes in Zingiberaceae—***

711 Certain characteristics of Zingiberaceae seeds have many character state reversals within
712 the family, creating a large number of homoplasious characters and character states, however
713 other characters show less homoplasy and are useful in separating formally recognized clades
714 (Table 3). The most useful characters for supporting currently recognized formal and informal
715 clades are those relating to the endotestal cells (31) and the type of chalazal pigment group (33),
716 also derived from the endotesta (Fig. 11). The endotesta has a single shift from thin and
717 parenchymatous in Siphonochiloideae and Zingiberoideae, to sclerified of various thicknesses in
718 Alpinioideae with no reversals to parenchymatous cells (Fig. 11). The chalazal pigment group
719 (33) are discoid in Siphonochiloideae and Zingiberoideae, but are non-discoid in Alpinioideae,
720 suggesting a single shift in Alpinioideae (Fig. 11). Trichomes on the seed coat or aril (3) have
721 perhaps been gained twice in Alpinioideae (*Siamanthus siliquosus* and *Siliquamomum*
722 *tonkinense*), and have been lost in at least three lineages in the Zingiberoideae (Fig. 12). Larsen

723 (2003) suggested that the trichomes found on some *Monolophus* create air pockets so they can be
724 abiotically dispersed by water, which would be an interesting ecological explanation for the
725 multiple originations of trichomes in Zingiberaceae seeds. The micropylar collar (15) was
726 previously shown by Liao and Wu (2000) to be lost in *Cautleya gracilis* and *Monolophus*
727 *coenobialis* Hance (as *Caulokaempferia coenobialis* (Hance) K.Larsen), which we confirm, and
728 we have documented additional instances of loss of micropylar collar (Fig. 12). It was lost at
729 least once in Globbeae (*Globba spathulata*), again in Zingibereae (*Camptandra ovata*), and in
730 Siphonochiloideae (Fig. 12). Interestingly all these seeds, except those of members of
731 Siphonochiloideae, are very small (1–2 mm), so the loss of the micropylar collar could be
732 attributed to reduction in seed size, but its absence in the large seeds of *Siphonochilus*
733 *aethiopicus* (>5 mm) refutes this idea. Loss of micropylar collar also does not correlate with the
734 loss of an operculum, because all taxa studied here without a micropylar collar still possess an
735 operculum. Further investigations into the functional roles of trichomes and the micropylar collar
736 are needed.

737 **Conclusions—**

738 Zingiberaceae seeds are morphologically and anatomically diverse and possess a large
739 number of systematically significant characters. Many of the characters used here are novel and
740 have the potential to be applied to other seed bearing plants with similar structural complexity.
741 The use of non-destructive SRXTM substantially increases confidence in the assessment of
742 characters because complications and artifacts arising from physical sectioning are avoided.
743 SRXTM also provides the ability to investigate rare and/or endangered taxa from herbaria, which
744 is useful for future studies centered on seed or fruit morphoanatomy as these are sometimes less

745 common in collections as compared with flowering specimens. Thirty-nine characters were
746 analyzed for 75 species within Zingiberaceae and 22 characters were found to be useful for
747 differentiating the subfamilies and tribes as currently described. Using a combination of
748 characters, the subfamilies Alpinioideae, Zingiberoideae, and Siphonochiloideae could each be
749 distinguished using seed morphoanatomy. Globbeae were the only tribe found to possess a
750 unique combination of character states not seen in any species outside the tribe. The lack of seed
751 character states that unite the other tribes may be due to a significant amount of homoplasy, but
752 seed features are still useful in combination with other morphological characters to determine
753 synapomorphies for the various clades, documenting the importance of widely surveying plant
754 groups for novel characters not previously used in classification studies. The seed character
755 states of currently unplaced genera within Zingiberaceae, *Monolophus* and *Siliquamomum*, have
756 been compared to those of other taxa within the family and suggest that *Siliquamomum* may be
757 related to Riedelieae, and *Monolophus* to Zingibereae. However, more data are needed in order
758 to formally revise the family. The Zingiberaceae are a large family with considerable
759 morphological and anatomical variation in both reproductive and vegetative characters. The
760 research presented here demonstrates the utility of using seed characters to independently test
761 hypotheses of evolutionary relationships. Further, morphological studies like this are critical to
762 understanding long-term evolutionary patterns where the fossil record will be considered, as no
763 DNA data are available for these extinct taxa.

764 **References**

765 BASKIN, C.C., AND BASKIN, J.M. 2001. Seeds, ecology, biogeography, and evolution of dormancy
766 and germination. Elsevier, San Diego, California, USA.

- 767 BENEDICT, J.C. 2012. Zingiberalean fossils from the Late Paleocene of North Dakota, USA and
768 their significance to the origin and diversification of Zingiberales. Ph.D. Dissertation, Arizona
769 State University, Tempe, Arizona, USA.
- 770 BENEDICT, J.C., S.Y. SMITH, M.E. COLLINSON, J. LEONG–ŠKORNIČKOVÁ, C.D. SPECHT, J.L. FIFE,
771 F. MARONE, X. XIAO, AND D.Y. PARKINSON. 2015. Evolutionary Significance of Seed Structure
772 in Alpinioideae (Zingiberaceae). *Botanical Journal of the Linnean Society* DOI:
773 10.1111/boj.12257.
- 774 BOESEWINKEL, F.D., AND F. BOUMAN. 1995. The Seed: Structure and Function. *In* J. Kigel, and G.
775 Galili [eds.], Seed development and germination, 1–24. Marcel Dekker, Inc., New York, New
776 York, USA.
- 777 BURTT, B.L., AND R.M. SMITH. 1972. Key species in the taxonomic history of Zingiberaceae.
778 *Notes from the Royal Botanical Garden Edinburgh* 177–227.
- 779 CHEN, I., AND S.R. MANCHESTER. 2007. Seed morphology of modern and fossil *Ampelocissus*
780 (Vitaceae) and implications for phytogeography. 2007. *American Journal of Botany* (94)9:
781 1534–1553.
- 782 COLLINSON, M.E., S.R. MANCHESTER, AND V. WILDE. 2012. Fossil fruits and seeds of the Middle
783 Eocene Messel biota, Germany. *Abhandlungen der Senckenberg Gesellschaft für Naturforschung*
784 570: 1–249.
- 785 COLLINSON M.E., AND P.F. VAN BERGEN. 2004. Evolution of angiosperm fruit and seed dispersal
786 biology and ecophysiology: morphological, anatomical and chemical evidence from fossils. *In*

- 787 A.R. Hemsley, and I. Poole [eds.], *The evolution of plant physiology*, Linnean society
788 symposium series no. 21, 323–377. Elsevier, London, UK.
- 789 CORNER, E.J.H. 1976. *The seeds of dicotyledons*, vols. 1 and 2. Cambridge University Press,
790 Cambridge, UK.
- 791 DOWD, B.A., G.H. CAMPBELL, R.B. MARR, V. NAGARKAR, S. TIPNIS, L. AXE, AND D.P. SIDONS.
792 1999. Developments in synchrotron x-ray computed microtomography at the National
793 Synchrotron Light Source. *Proceedings of SPIE 3772*: 224–236.
- 794 GROOTJEN, C.J., AND F. BOUMAN. 1981. Development of the ovule and seed in *Costus cuspidatus*,
795 with special reference to the formation of the operculum. *Botanical Journal of the Linnean*
796 *Society* 83: 27–39.
- 797 HARRIS, D.J., A.D. POULSEN, C. FRIMODT-MØLLER, J. PRESTON, AND Q.C.B. CRONK. 2000. Rapid
798 radiation in *Aframomum* (Zingiberaceae): evidence from nuclear ribosomal DNA internal
799 transcribed spacer (ITS) sequences. *Edinburgh Journal of Botany* 57: 377–395.
- 800 HERRERA, F., S.R. MANCHESTER, M.R. CARVALHO, C. JARAMILLO, AND S.L. WING. 2014.
801 Paleocene wind-dispersed fruits and seeds from Colombia and their implications for early
802 Neotropical rainforests. *Acta Palaeobotanica* 54(2): 197–229.
- 803 HOLTUM, R.E. 1950. The Zingiberaceae of the Malay Peninsula. *Gardener's Bulletin of*
804 *Singapore* 13: 1–249.
- 805 HUMPHREY, J.E. 1896. The development of the seed in the Scitamineae. *Annals of Botany* 37: 1–
806 40.

- 807 KAPIL, R.N., J. BOR, AND F. BOUMAN. 1980. Seed appendages in Angiosperms. I. Introduction.
808 *Botanische Jahrbücher für Systematik, Pflanzengeschichte und Pflanzengeographie* 101: 555–
809 573
- 810 KRESS, W.J. 1996. Phylogeny of the Zingiberanae: Morphology and molecules. *In* T.L. Wu, Q.G.
811 Wu, and Z.Y. Chen [eds.], Proceedings of the 2nd Symposium on the Family Zingiberaceae,
812 122–141. Zhongshan University Press, Guangzhou, China.
- 813 KRESS, W.J., L.M. PRINCE, W.J. HAHN, AND E.A. ZIMMER. 2001. Unraveling the evolutionary
814 radiation of the families of Zingiberales using morphological and molecular evidence. *Systematic*
815 *Biology* 50: 926–944.
- 816 KRESS, W.J., L.M. PRINCE, AND K.J. WILLIAMS. 2002. The phylogeny and a new classification of
817 the gingers (Zingiberaceae): evidence from molecular data. *American Journal of Botany* 89:
818 1682–1696.
- 819 KRESS, W.J., A-Z. LIU, M. NEWMAN, AND Q-J. LI. 2005. The molecular phylogeny of *Alpinia*
820 (Zingiberaceae): a complex and polyphyletic genus of gingers. *American Journal of Botany* 92:
821 167–178.
- 822 KRESS, W.J., M.F. NEWMAN, A.D. POULSEN, AND C.D. SPECHT. 2007. An analysis of generic
823 circumscriptions in tribe Alpinieae (Alpinioideae: Zingiberaceae). *Gardens' Bulletin Singapore*
824 59: 113–128.
- 825 LARSEN, K. 2003. Three new species of *Caulokaempferia* (Zingiberaceae) from Thailand with a
826 discussion of the generic diversity. *Nordic Journal of Botany* 22: 409-417.

- 827 LARSEN, K. 2005. Distribution patterns and diversity centres of Zingiberaceae in SE Asia.
828 *Biologiske Skrifter* 55: 219–228.
- 829 LARSEN, K., J.M. LOCK, H. MAAS, AND P.M.J. MASS. 1998. Zingiberaceae. In K. Kubitzki, [ed.],
830 The families and genera of vascular plants, vol. 4, Moncotyledons: Alismatanae to
831 Commelinanae (except Gramineae), 474–495. Springer, Berlin, Germany.
- 832 LARSEN, K., AND J. MOOD. 1998. *Siamanthus*, a new genus of Zingiberaceae from Thailand.
833 *Nordic Journal of Botany* 18: 393–397.
- 834 LARSEN, K., AND R.M. SMITH. 1972. Notes on *Caulokaempferia*. *Notes from the Royal Botanic*
835 *Garden Edinburgh* 31: 287–295.
- 836 LEONG-ŠKORNIČKOVÁ, J., L. NGOC-SÂM, A.D. POULSEN, J. TOSH, AND A. FORREST. 2011.
837 *Newmania*: A new ginger genus from central Vietnam. *Taxon* 60(5): 1386-1396.
- 838 LEONG-ŠKORNIČKOVÁ, J., O. ŠÍDA, E. ZÁVESKÁ, AND K. MARHOLD. 2015. History of infrageneric
839 classification, typification of supraspecific names and outstanding transfers in *Curcuma*
840 (Zingiberaceae). *Taxon* 64(2): 362-373.
- 841 LIAO, J.P., AND Q.G. WU. 1996. The significance of the seed anatomy of Chinese *Alpinia*. In T.L.
842 Wu, Q.G. Wu, and Z.Y. Chen [eds.], Proceedings of the 2nd Symposium on the Family
843 Zingiberaceae, 92–106. Zhongshan University Press, Guangzhou, China.
- 844 LIAO, J.P., AND Q.G. WU. 2000. A preliminary study of the seed anatomy of Zingiberaceae.
845 *Botanical Journal of the Linnean Society* 134: 287–300.

- 846 MACDOWELL, A.A., D.Y. PARKINSON, A. HABOUB, E. SCHAIBLE, J.R. NASIATKA, C.A. YEE, J.R.
847 JAMESON, J.B. AJO-FRANKLIN, C.R. BRODERSEN, AND A.J. MCELRONE. 2012. X-ray micro-
848 Tomography at the Advanced Light Source. *Proceedings of SPIE* 8506: 850618.
- 849 MADDISON, W.P., AND D.R. MADDISON. 2015. Mesquite: a modular system for evolutionary
850 analysis. Version 3.03 for Windows. Computer program and documentation distributed by the
851 authors, website <http://mesquiteproject.org> [accessed 30 April 2015].
- 852 MANCHESTER, S.R., AND W.J. KRESS. 1993. *Ensete oregonense* sp. nov. from the Eocene of
853 western North America and its phylogeographic significance. *American Journal of Botany* 80:
854 1264–1272. MARONE, F., B. MÜNCH, AND M. STAMPANONI. 2010. Fast reconstruction algorithm
855 dealing with tomography artifacts. *SPIE Proceedings ‘‘Developments in X-Ray Tomography VII’’*
856 7804: 780410.
- 857 MARONE, F., AND M. STAMPANONI. 2012. Regridding reconstruction algorithm for real-time
858 tomographic imaging. *Journal of Synchrotron Radiation* 19: 1029–1037.
- 859 MAURITZON, J. 1936. Samenbau und Embryologie einiger Scitamineen. *Lunds Universitets*
860 *Arsskrift* 31: 1–31.
- 861 MOOD, J.D. 1996. The native gingers of Sabah. *Bulletin of the Heliconia Society International* 8
862 (3/4): 1–8.
- 863 MOOD, J.D., J.F. VELDKAMP, S. DEY, AND L.M. PRINCE. 2014. Nomenclatural changes in
864 Zingiberaceae: *Caulokaempferia* is a superfluous name for *Monolophus* and *Jirawongsea* is
865 reduced to *Boesenbergia*. *Gardens’ Bulletin Singapore* 66(2): 215–231.

- 866 NETOLITZKY, F. 1926. Anatomie der Angiospermen-Samen. *In* K. Linsbauer [ed.], Handbuch
867 Pflanzen Anatomie. vol. 10, 1–364. Gebrüder Borntraeger, Berlin, Germany.
- 868 NGAMRIABSAKUL, C., M.F. NEWMAN, AND Q.C.B. CRONK. 2004. The phylogeny of tribe
869 Zingibereae (Zingiberaceae) based on ITS (nrDNA) and *trnL-F* (cpDNA) sequences. *Edinburgh*
870 *Journal of Botany* 60(3): 483–507.
- 871 PEDERSEN, L.B. 2004. Phylogenetic analysis of the subfamily Alpinioideae (Zingiberaceae),
872 particularly *Etilingera* Giseke, based on nuclear and plastid DNA. *Plant Systematics and*
873 *Evolution* 245: 239–258.
- 874 RANGSIRUJI, A., M.F. NEWMAN, AND Q.C.B. CRONK. 2000. A study of the infrgeneric
875 classification of *Alpina* (Zingiberaceae) based on the ITS region of nuclear rDNA and the *trnL-F*
876 spacer of chloroplast DNA. *In* K.L. Wilson and D.A. Morrison [eds.], *Monocots — Systematics*
877 *and Evolution*, 695–709. CSIRO Publishing, Collingwood, Australia.
- 878 RIDLEY, H.N. 1909. Fruit of *Burbidgea*. *Journal of the Straits Branch of the Royal Asiatic*
879 *Society* 53: 175–176.
- 880 SCHUMANN, K. 1904. Zingiberaceae. *Das Pflanzenreich* 4: 1–458.
- 881 SMITH, S.Y., M.E. COLLINSON, P.J. RUDALL, D.A. SIMPSON, F. MARONE, AND M. STAMPANONI.
882 2009. Virtual taphonomy using synchrotron tomographic microscopy reveals cryptic features and
883 internal structure of modern and fossil plants. *Proceedings of the National Academy of Sciences*
884 *of the United States of America* 106(29): 12013–12018.
- 885 SIMPSON, M.G. 2010. *Plant Systematics*, 2nd ed. Elsevier Publishing, Amsterdam, Netherlands.

- 886 STAMPANONI, M., A. GROSO, A. ISENEGGER, G. MIKULJAN, Q. CHEN, A. BERTRAND, S. HENEIN, R.
887 BETEMPS, U. FROMMHERZ, P. BÖHLER, D. MEISTER, M. LANGE, AND R. ABELA. 2006. Trends in
888 synchrotron-based tomographic imaging: the SLS experience. *Proceedings of SPIE* 6318:
889 63180M.
- 890 TAKHTAJAN, A. 1985. Comparative anatomy of seeds, vol I., 1–318. Izdat Nauka, Leningrad,
891 Russia.
- 892 TSCHIRCH, A. 1891. Physiologische Studien über die Samen, insbesondere die Saugorgane
893 derselben. *Annales du Jardin botanique de Buitenzorg* 8(1): 143–145.
- 894 THE INTERNATIONAL PLANT NAMES INDEX (2015). Website <http://www.ipni.org> (accessed 22
895 May 2015).
- 896 THE PLANT LIST. 2013. Version 1.1. Website <http://www.theplantlist.org/> (accessed 22 May
897 2015).
- 898 THIERS, B. [continuously updated]. Index Herbariorum: A global directory of public herbaria and
899 associated staff. New York Botanical Garden's Virtual Herbarium. <http://sweetgum.nybg.org/ih/>
900 [01 January 2015]
- 901 VAUGHAN, J.G. 1970. The Structure and Utilization of Oil Seeds. Chapman and Hall LTD,
902 London, UK.
- 903 WADA, S., J.A. KENNEDY, AND B.M. REED. 2011. Seed-coat anatomy and proanthocyanidins
904 contribute to the dormancy of *Rubus* seed. *Scientia Horticulturae* 130: 762–768.

905 WILLIAMS, K.J., W.J. KRESS, AND P.S. MANOS. 2004. The phylogeny, evolution and classification
906 of the genus *Globba* and tribe Globbeae (Zingiberaceae): Appendages do matter. *American*
907 *Journal of Botany* 91: 100–114.

908 WOOD, T.H., W.M. WHITTEN, AND N.H. WILLIAMS. 2000. Phylogeny of *Hedychium* and related
909 genera (Zingiberaceae) based on ITS sequence data. *Edinburgh Journal of Botany* 57(2): 261–
910 270.

911 WU, Q.G., AND J.P. LIAO. 1995. Anatomy and histochemistry of the seeds of *Amomum villosum*.
912 *Journal of Tropical and Subtropical Botany* 3: 52–59.

913 XIA, Y.M., KRESS W.J., AND PRINCE L.M. 2004. A phylogenetic analysis of *Amomum*
914 (Alpinioideae: Zingiberaceae) using ITS and *matK* DNA sequence data. *Systematic Botany* 29:
915 334–344.

916 ZÁVESKÁ, E., T. FÉR, O. ŠÍDA, K. KRAK, K. MARHOLD, AND J. LEONG–ŠKORNIČKOVÁ. 2012.
917 Phylogeny of *Curcuma* (Zingiberaceae) based on plastid and nuclear sequences: Proposal of the
918 new subgenus *Ecomata*. *Taxon*. 61(4): 747–763.

919

920 Table 1. Currently recognized subfamilies, tribes, and genera within Zingiberaceae (after Kress
 921 et al., 2002; Takano and Nagamasu, 2007; Kress et al., 2010; Leong-Škorničková et al., 2011;
 922 Mood et al., 2014). Numbers in parentheses indicate currently accepted number of species
 923 reported on The Plant List (2013), IPNI (2015), in Mood et al. (2014), or Leong-Škorničková et
 924 al. (2015).(*) denotes genera described since Kress et al. (2002).

Subfamily Siphonochiloideae	Subfamily Tamijioideae	Subfamily Alpinioideae	Subfamily Zingiberoideae
Tribe Siphonochileae	Tribe Tamijieae	Tribe Alpinieae	Tribe Zingibereae
<i>Aulotandra</i> (6) <i>Siphonochilus</i> (11)	<i>Tamijia</i> (1)	<i>Aframomum</i> (56) <i>Alpinia</i> (247) <i>Amomum</i> (180) <i>Cyphostigma</i> (1) <i>Elettaria</i> (11) <i>Elettariopsis</i> (20) <i>Etilingera</i> (100) <i>Geocharis</i> (6) <i>Geostachys</i> (25) <i>Hornstedtia</i> (34) <i>Leptosolena</i> (1) <i>Plagiostachys</i> (27) <i>Renealmia</i> (87) <i>Vanoverberghia</i> (2)	<i>Boesenbergia</i> (69) <i>Camptandra</i> (4) <i>Cautleya</i> (2) <i>Cornukaempferia</i> (3) <i>Curcuma</i> (105) <i>Distichochlamys</i> (3) <i>Haniffia</i> (4) <i>Haplochorema</i> (6) <i>Hedychium</i> (95) <i>Kaempferia</i> (36) <i>Larsenianthus</i> * (4) <i>Nanochilus</i> (1) <i>Newmania</i> * (2) <i>Myxochlamys</i> * (2) <i>Parakaempferia</i> (1) <i>Pommereschea</i> (2) <i>Rhynchanthus</i> (4) <i>Roscoea</i> (23) <i>Scaphochlamys</i> (34) <i>Stadiochilus</i> (1) <i>Zingiber</i> (146)
		Tribe Riedelieae <i>Burbidgea</i> (5) <i>Pleuranthodium</i> (23) <i>Riedelia</i> (75) <i>Siamanthus</i> (1)	Tribe Globbeae <i>Gagnepainia</i> (3) <i>Globba</i> (106) <i>Hemiorchis</i> (3)
		Incertae Sedis <i>Siliquamomum</i> (3)	Incertae Sedis <i>Monolophus</i> (25)

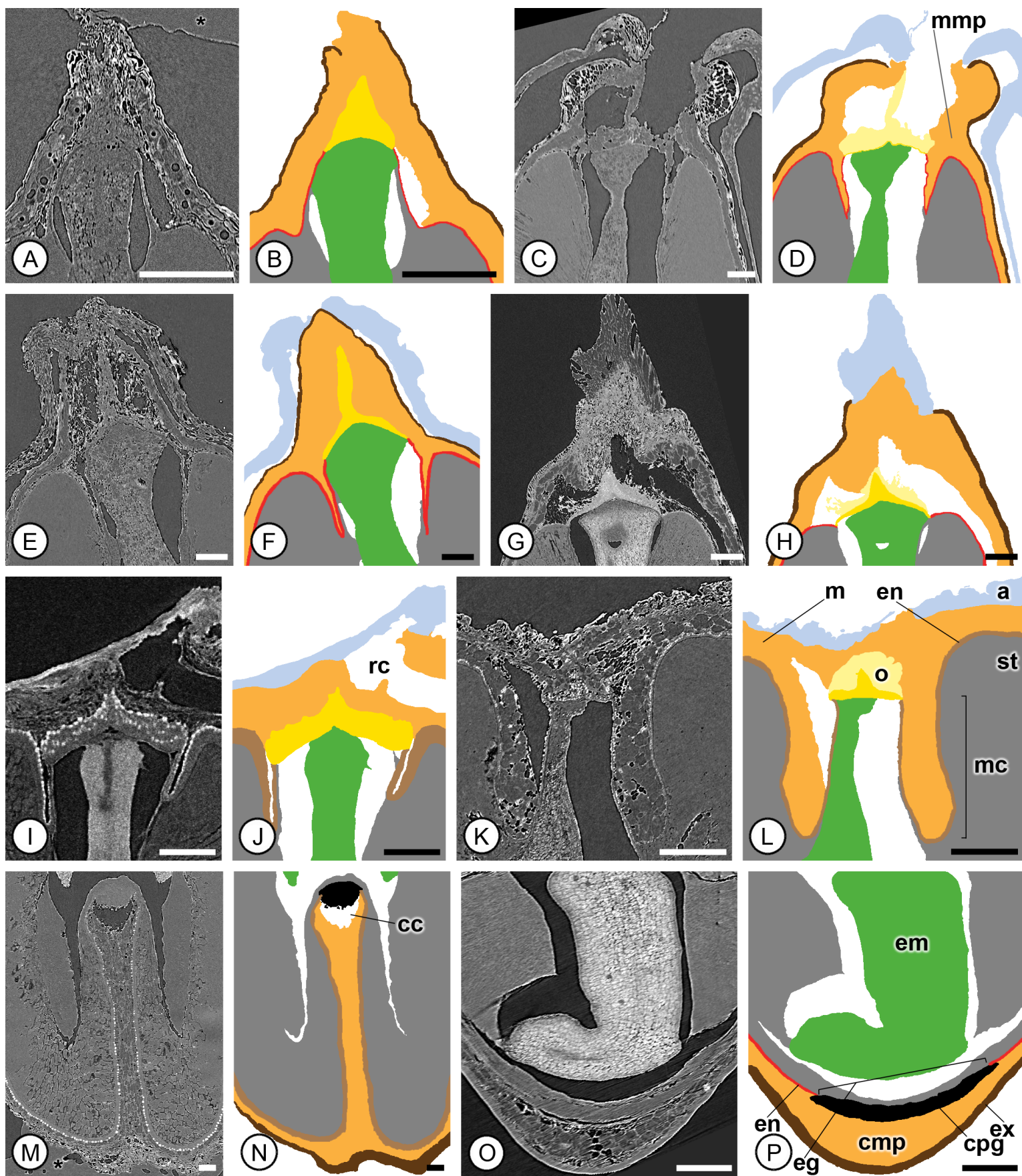
925 Table 2. List of specimens sampled and their voucher information. Herbarium abbreviations
 926 follow Index Herbariorum (Thiers, continually updated). Numbers in parentheses indicate
 927 number and type of specimens scanned per taxon.

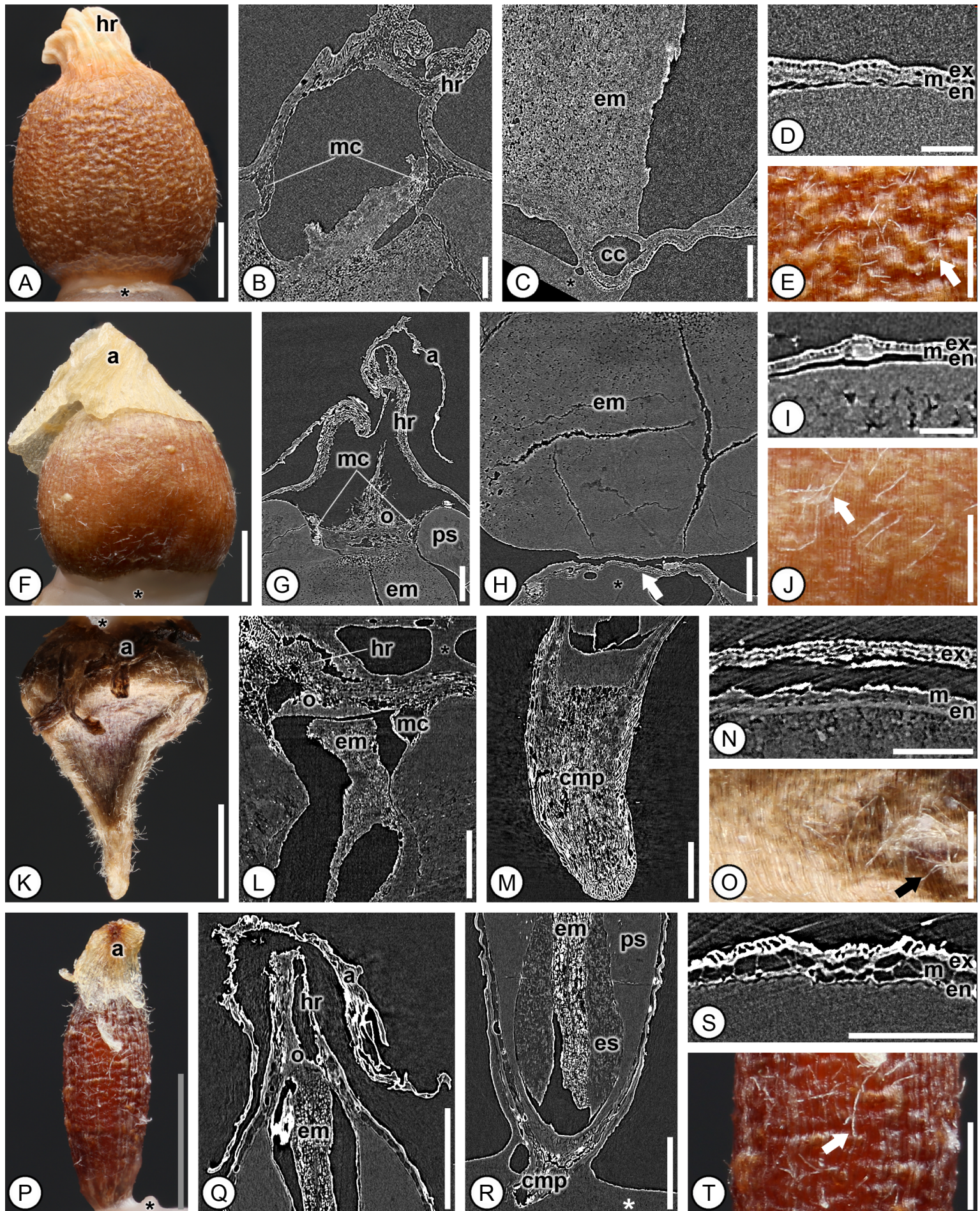
Species	Voucher Information
<i>Aframomum chrysanthum</i> Lock	SING, GRC–173 (1 seed)
<i>Aframomum daniellii</i> (Hook.f.) K.Schum.	Delft University of Technology, JW van Loon (1 seed)
<i>Aframomum melegueta</i> K.Schum.	US, J. Higgins 44 (1 seed)
<i>Alpinia aquatica</i> (Retz.) Roscoe	SING, GRC–22, and US, WJ Kress 05–7809 (2 seeds and 1 fruit)
<i>Alpinia boia</i> Seem.	US, WJ Kress 79–1071, and US, AC Smith 4087 (2 seeds)
<i>Alpinia brevilabris</i> C.Presl	US, M Ramos 30411 (1 seed)
<i>Alpinia caerulea</i> (R.Br.) Benth.	SING, JLS–1660 (1 seed)
<i>Alpinia carolinensis</i> Koidz.	US, DH Lorence 7907 (1 seed)
<i>Alpinia conchigera</i> Griff.	SING, GRC–205 (1 seed)
<i>Alpinia fax</i> (Thwaites) B.L.Burt & R.M.Sm.	US, AHM Jayasuriya 1217 (1 seed and 1 fruit)
<i>Alpinia galanga</i> (L.) Willd.	US, Shiu Ying Hu 6225 (1 seed and 1 fruit)
<i>Alpinia haenkei</i> C.Presl	US, ADE Elmer 17662 (1 seed)
<i>Alpinia japonica</i> (Thunb.) Miq.	NY, Muratailcitamura 639 (1 seed)
<i>Alpinia javanica</i> Blume	SING, Umbai and Millard 1430 (1 seed)
<i>Alpinia luteocarpa</i> Elmer	US, Kress and Li 05–7785 (1 seed)
<i>Alpinia malaccensis</i> (Burm.f.) Roscoe	US, C Saldanha 14771 (1 seed)

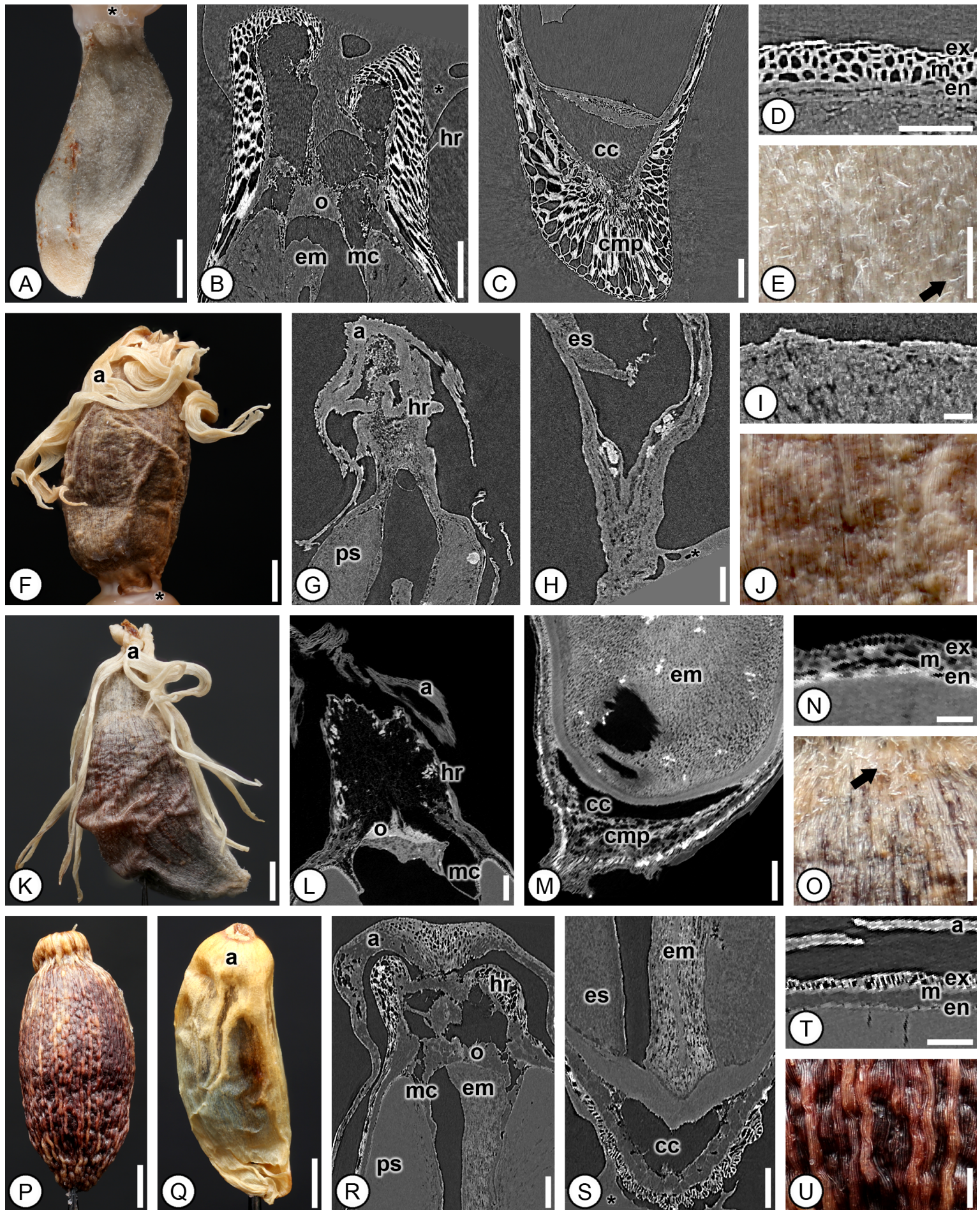
<i>Alpinia nigra</i> (Gaertn.) B.L.Burtt	US, WJ Kress 00–6808 (1 seed)
<i>Alpinia oceanica</i> Burkill	E, Stone and Streimann 10296 (1 seed)
<i>Alpinia purpurata</i> (Vieill.) K.Schum.	E, AN Miller NGF 38482 (1 seed)
<i>Alpinia rafflesiana</i> Wall. ex Baker	SING, Ridley s.n. (1 seed)
<i>Alpinia stachyodes</i> Hance	US, n.c., 1801 (1 seed)
<i>Alpinia zerumbet</i> (Pers.) B.L.Burtt & R.M.Sm.	US, Wen 9412, and US, Fosberg 38289 (2 seeds)
<i>Amomum koenigii</i> J.F.Gmel.	SING, VNM–B–1443 (1 seed)
<i>Amomum lappaceum</i> Ridl.	SING, JLS–1667 (1 seed)
<i>Amomum ochreum</i> Ridl.	SING, JLS–1670 (1 seed)
<i>Amomum sericeum</i> Roxb.	SING, JLS–1273 (1 seed)
<i>Aulotandra trigonocarpa</i> H.Perrier	K, M Bardot–Vaucoulon 1272 (1 fruit)
<i>Boesenbergia curtisii</i> (Baker) Schltr.	NY, Henderson 22874 (1 seed)
<i>Burbridgea stenantha</i> Ridl.	SING, GRC–88 (1 seed)
<i>Camptandra ovata</i> Ridl.	JLS–1669 (1 seed)
<i>Cautleya gracilis</i> (Sm.) Dandy	MO, K Larsen 46744 (2 seeds and 1 fruit)
<i>Cautleya spicata</i> (Sm.) Baker	MICH, JC Benedict s.n. (commercially purchased) (1 seed)
<i>Curcuma montana</i> Roxb.	SING, JLS–73474 (1 seed)
<i>Curcuma pierreana</i> Gagnep.	SING, Ly–489 (1 seed)
<i>Distichochlamys citrea</i> M.F.Newman	SING, JLS–1615 (1 seed)
<i>Elettariopsis unifolia</i> (Gagnep.) M.F.Newman	MO, JF Maxwell 00–390 (1 seed)
<i>Etlingera elatior</i> (Jack) R.M.Sm.	SING, SNG–56 (1 seed)

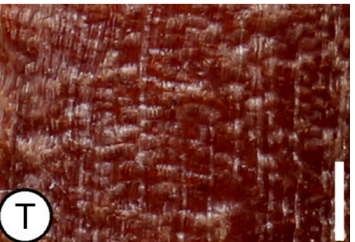
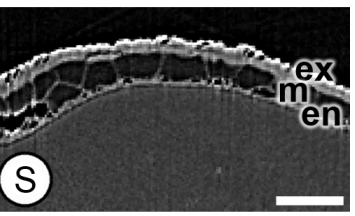
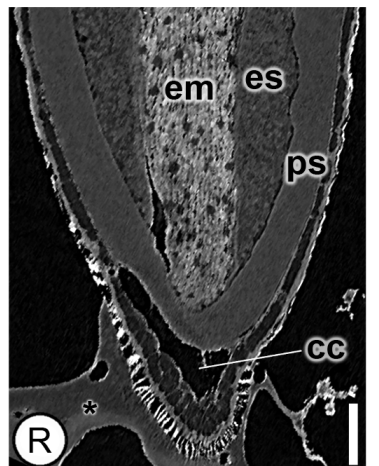
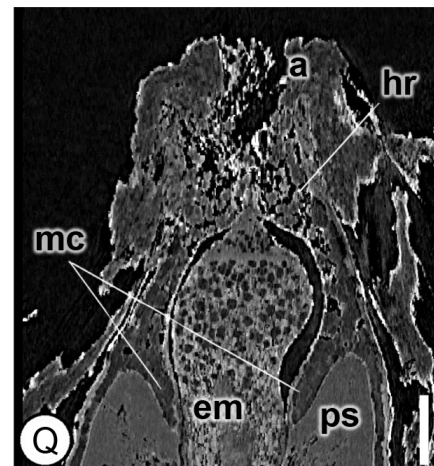
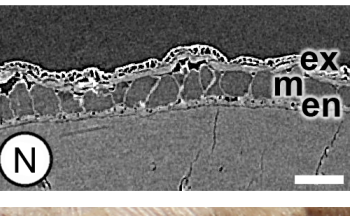
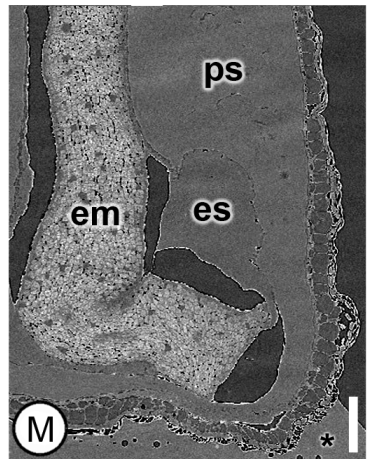
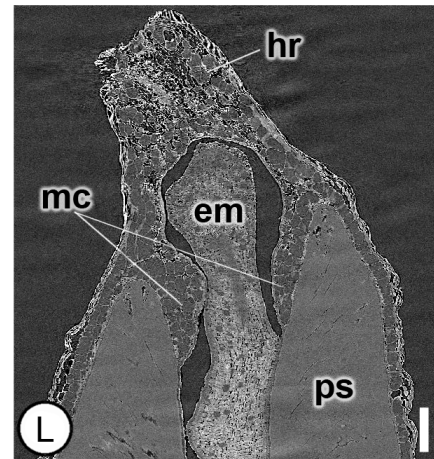
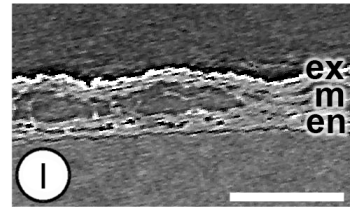
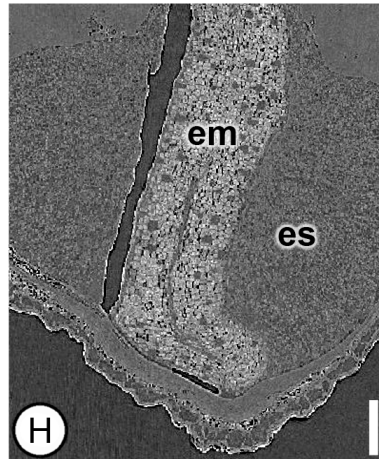
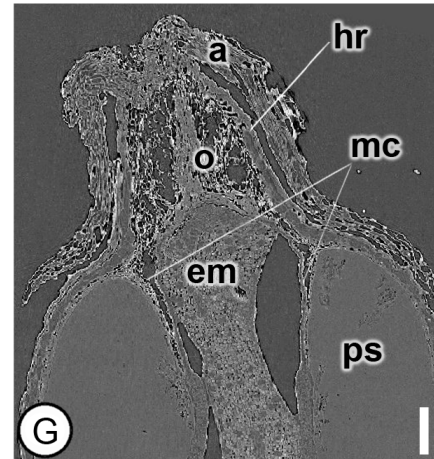
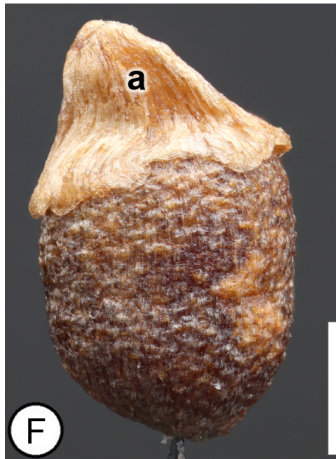
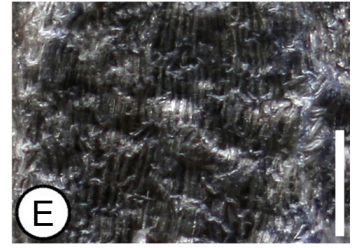
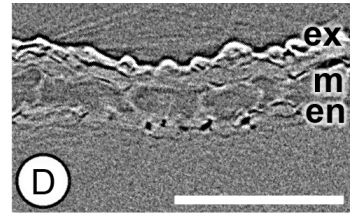
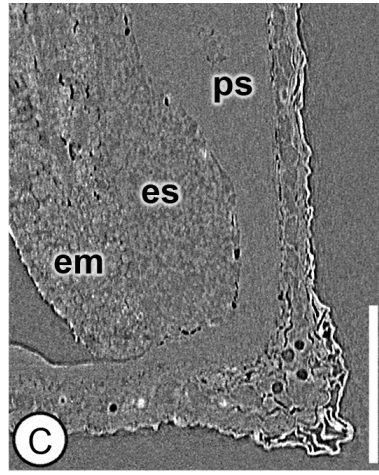
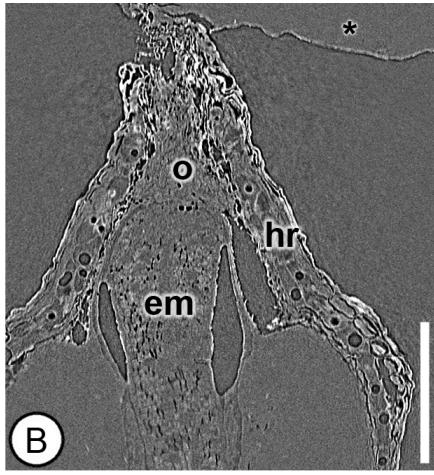
<i>Etilingera linguiformis</i> (Roxb.) R.M.Sm.	US, WJ Kress, M Bordelon, T Htum 02–7044 (1 seed)
<i>Etilingera yunnanensis</i> (T.L.Wu & S.J.Chen) R.M.Sm.	SING, JLS–1717 (1 seed)
<i>Gagnepainia harmandii</i> (Baill.) K.Schum.	SING, GRC–132 (1 seed)
<i>Geocharis aurantiaca</i> Ridl.	SING, Corner 32777 (1 seed)
<i>Geostachys densiflora</i> Ridl.	SING, JLS–1662 (1 seed)
<i>Globba aurea</i> Elmer	MICH, HH Bartlett 15543 (1 seed)
<i>Globba maculata</i> Blume	MICH, HH Bartlett 7544 (1 seed)
<i>Globba pendula</i> Roxb.	NYBG, Rahmat Si Toroes 3668 (1 seed)
<i>Globba sessiliflora</i> Sims	SING, JLS–1957 (1 seed)
<i>Globba spathulata</i> Roxb.	US, WJ Kress 01–6914 (1 seed)
<i>Hedychium coronarium</i> J.Koenig	MICH, A Shilom Tan 1771 (1 seed)
<i>Hedychium gardnerianum</i> Sheppard ex Ker Gawl.	MICH, SY Smith s.n. (commercially purchased) (1 seed)
<i>Hedychium hasseltii</i> Blume	US, T Wood 94–3700 (1 seed)
<i>Hedychium muluense</i> R.M.Sm.	SING, JLS–54 (1 seed)
<i>Hemiorchis</i> sp.	US, WJ Kress 01–6884 (1 seed)
<i>Hornstedtia conica</i> Ridl.	SING, SNG–35 (1 seed)
<i>Hornstedtia leonurus</i> (J.Koenig) Retz.	SING, SNG–174 (1 seed)
<i>Hornstedtia scottiana</i> (F.Muell.) K.Schum.	US, WJ Kress 80–1129 (1 seed)
<i>Kaempferia pulchra</i> Ridl.	K, Rabil 296 (1 seed)

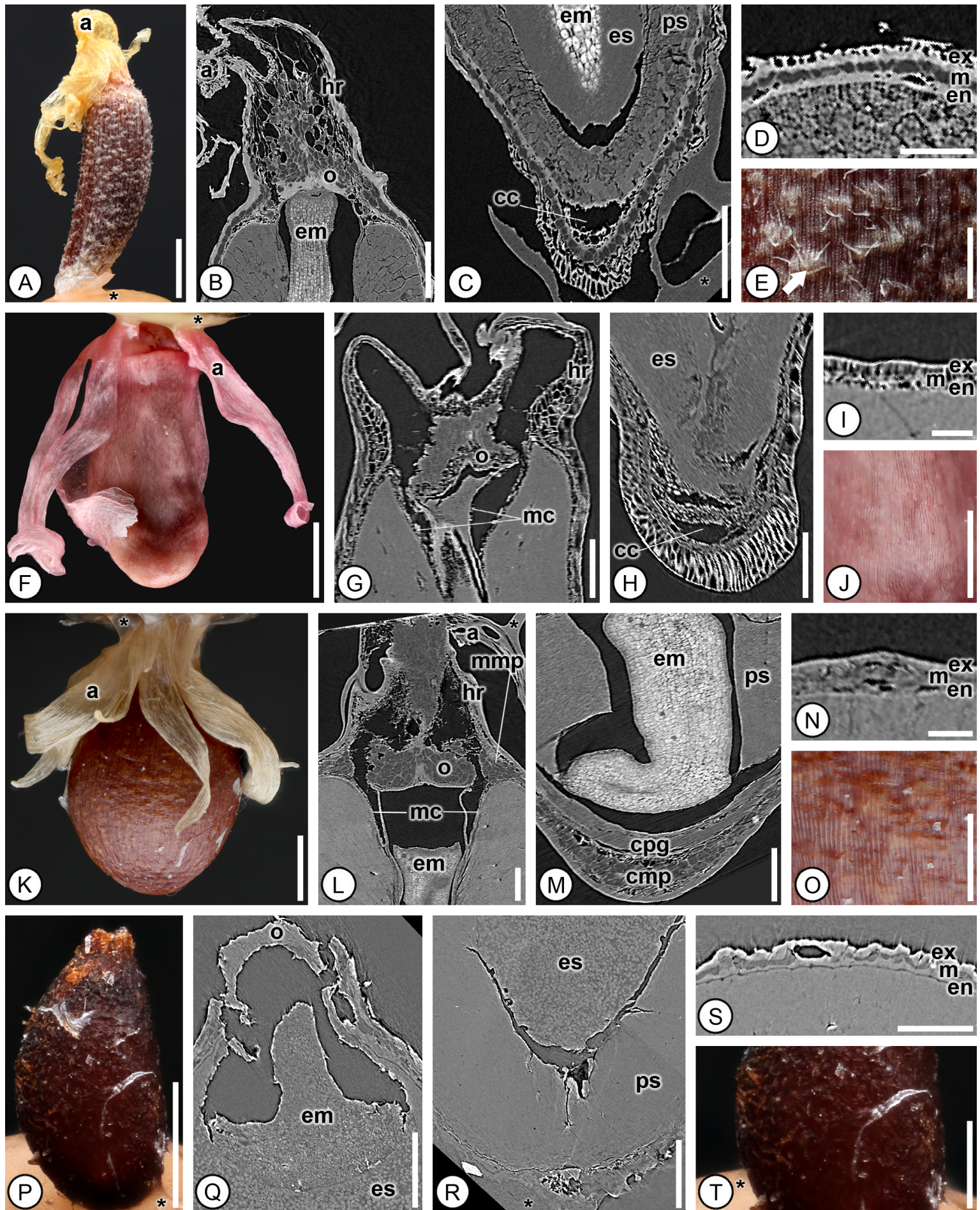
<i>Monolophus sikkimensis</i> (King ex Baker) Veldkamp & Mood	SING, Wallich s.n. (1 seed)	928 929
<i>Newmania</i> sp.	SING, JLS-1646 (1 seed)	930
<i>Plagiostachys escritorii</i> Elmer	NY, Elmer 16216 (1 seed)	931
<i>Plagiostachys philippinensis</i> Ridl.	NY, Ramos and Edaño 75626 (1 seed)	932
<i>Pleuranthodium</i> sp.	US, TG Hartley 10989 (1 seed)	933
<i>Renealmia lucida</i> Maas	SING, JLS-1019 (1 seed)	934
<i>Renealmia occidentalis</i> (Sw.) Sweet	MICH, J Vera Santos 2513 (1 seed)	935
<i>Riedelia corallina</i> (K.Schum.) Valetton	NY, Annable 3639 (1 seed)	936
<i>Riedelia</i> sp.	SING, JLS-428 (1 seed)	937
<i>Roscoea alpina</i> Royle	AAU, 1013 (1 seed)	938
<i>Siamanthus siliquosus</i> K.Larsen & Mood	US, WJ Kress 99-6358 (1 seed)	939
<i>Siliquamomum tonkinense</i> Baill.	SING, VNM-B-1469 (1 seed)	940
<i>Siphonochilus aethiopicus</i> (Schweinf.) B.L.Burt	MO, P Kuchar 22948 (1 seed and 1 fruit)	941 942
<i>Siphonochilus kirkii</i> (Hook.f.) B.L.Burt	MO, ABKatende K1880 (2 seeds)	943
<i>Vanoverberghia sepulchrei</i> Merr.	NY, Ramos and Edaño 45045 (1 seed and 1 fruit)	944 945
<i>Zingiber larsenii</i> Theilade	SING, JLS-1270 (1 seed)	946
<i>Zingiber officinale</i> Roscoe	Delft University of Technology, JW van Loon (1 seed)	947
<i>Zingiber spectabile</i> Griff.	Delft University of Technology, JW van Loon (1 seed)	948 949
<i>Zingiber thorelii</i> Gagnep.	SING, JLS-1271 (1 seed)	

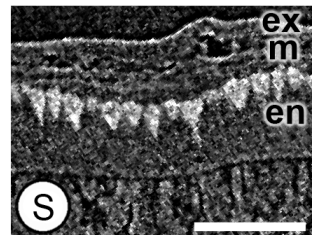
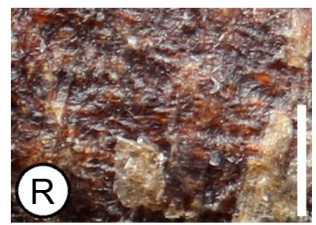
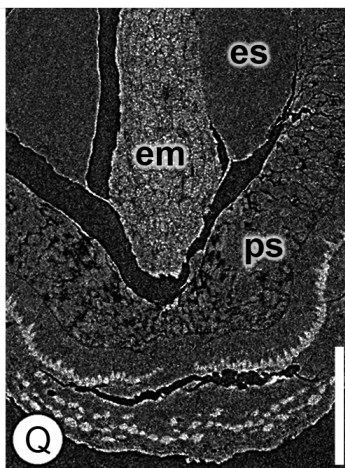
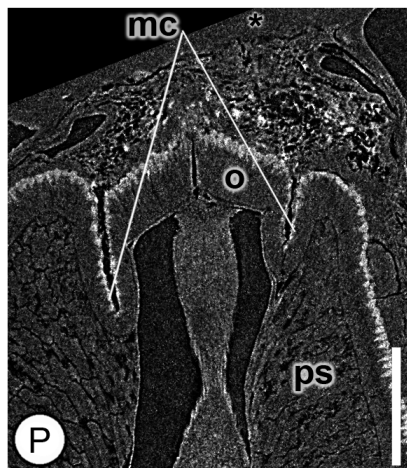
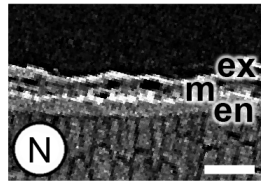
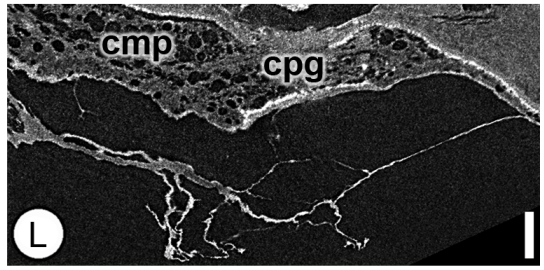
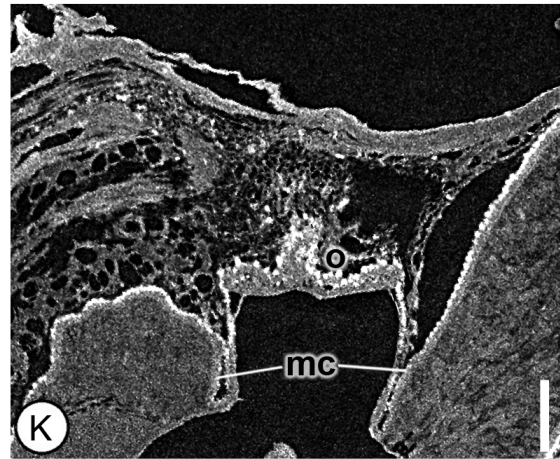
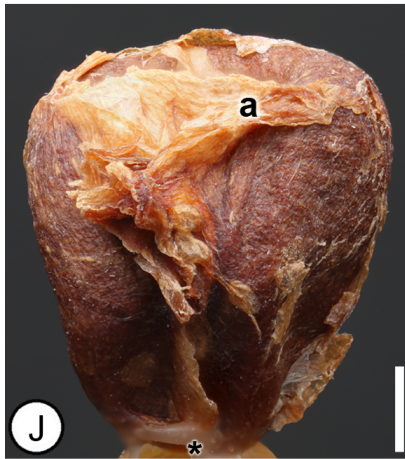
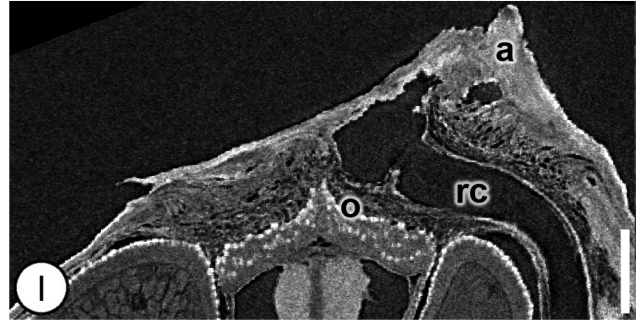
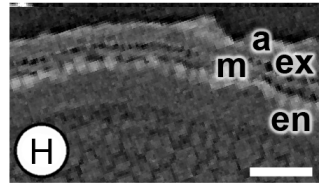
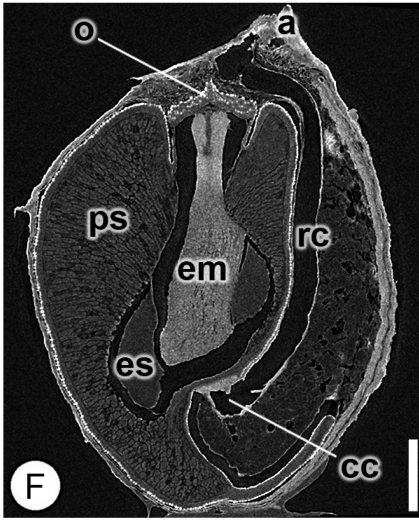
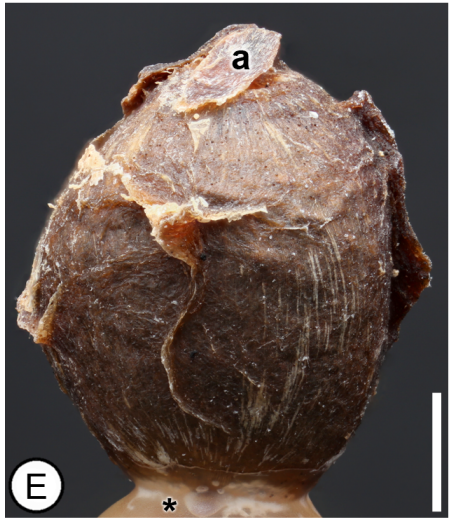
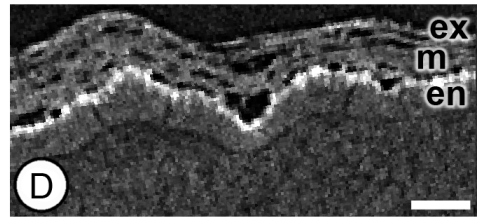
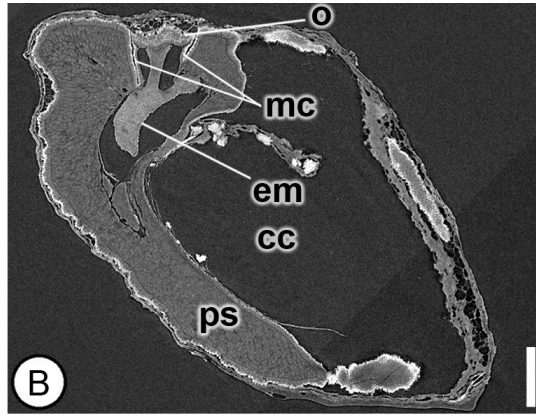


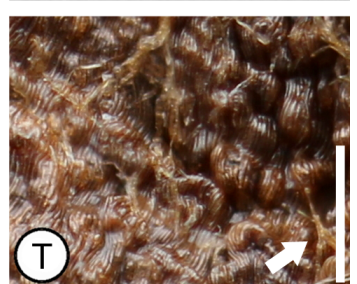
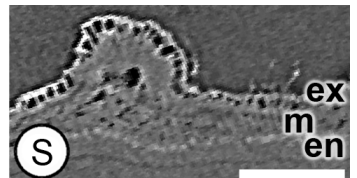
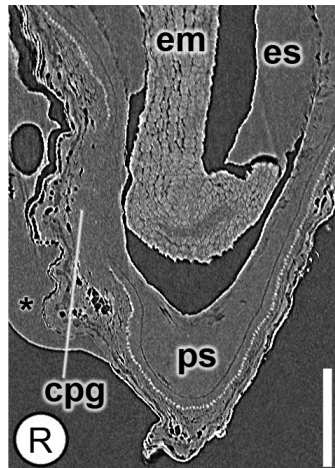
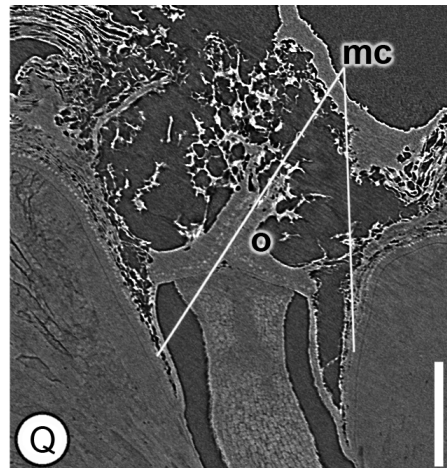
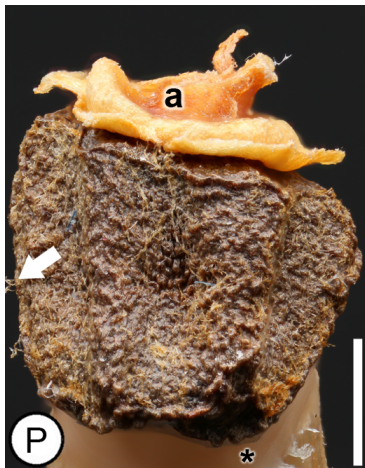
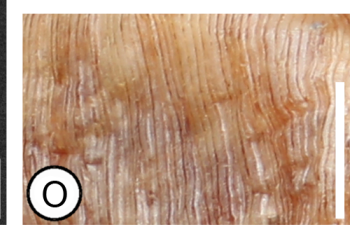
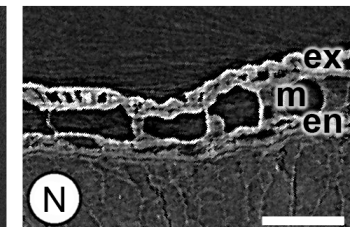
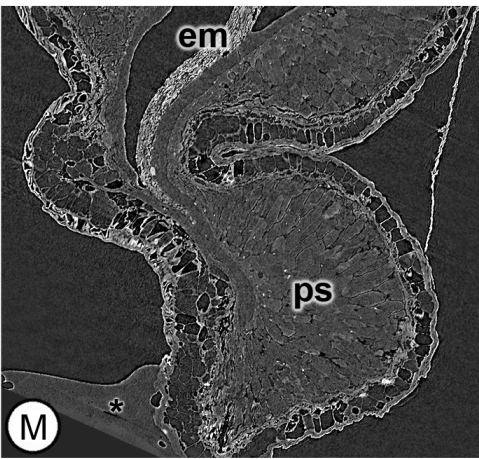
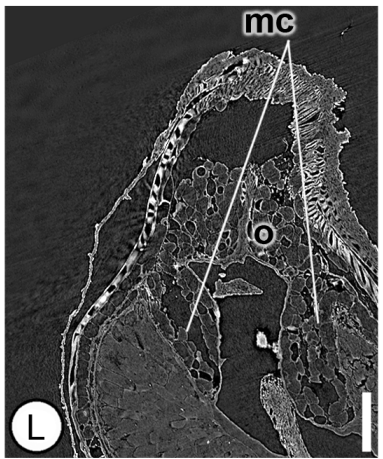
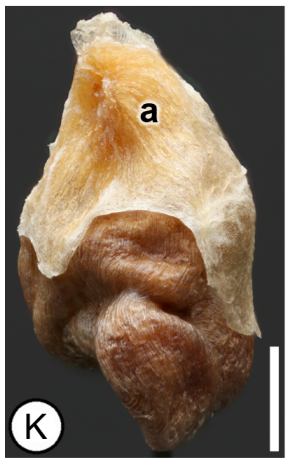
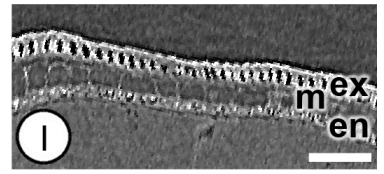
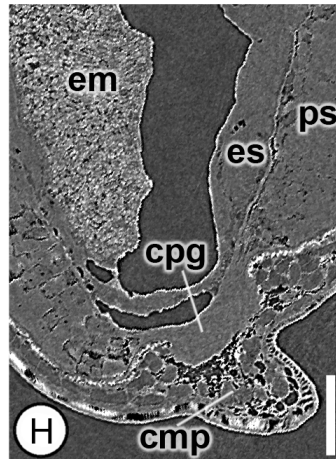
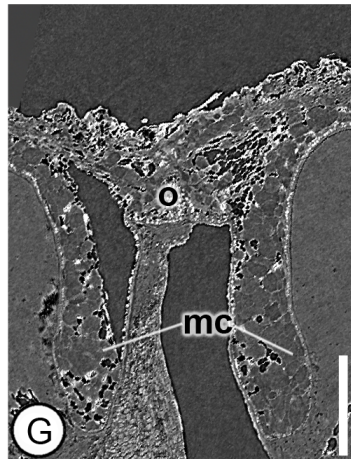
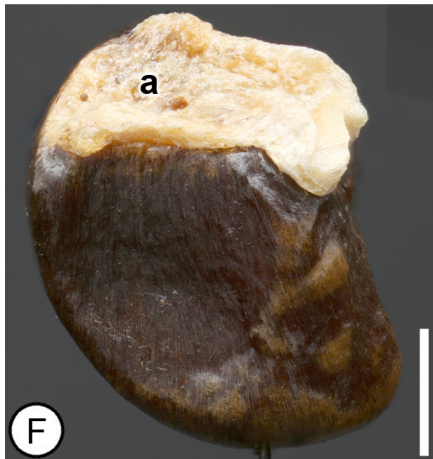
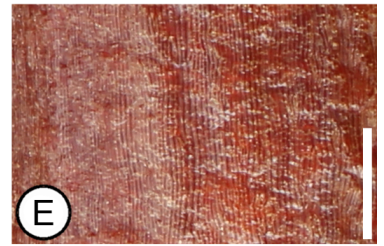
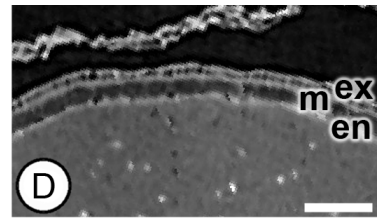
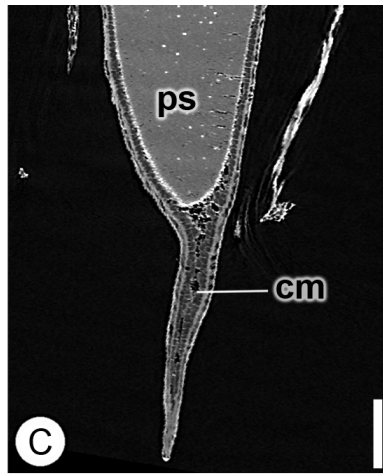
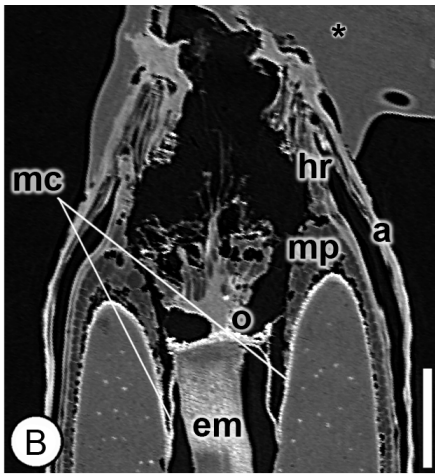


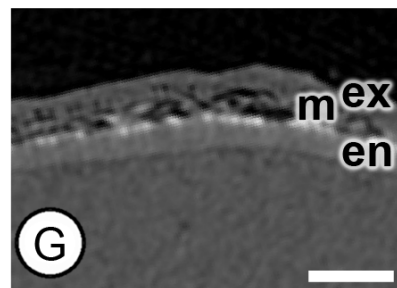
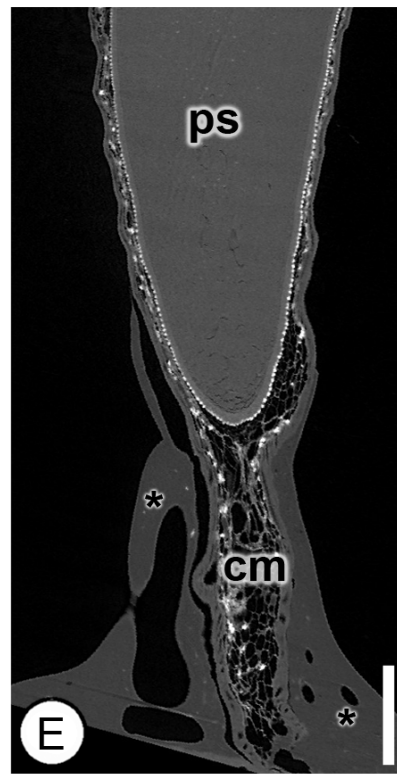
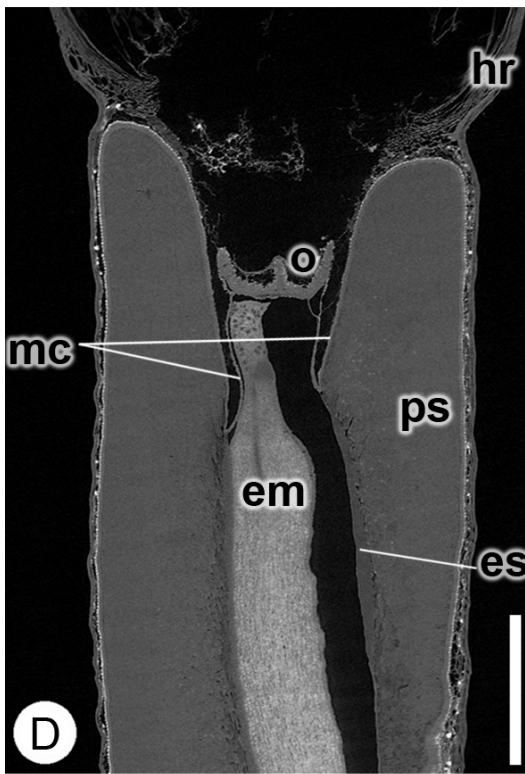
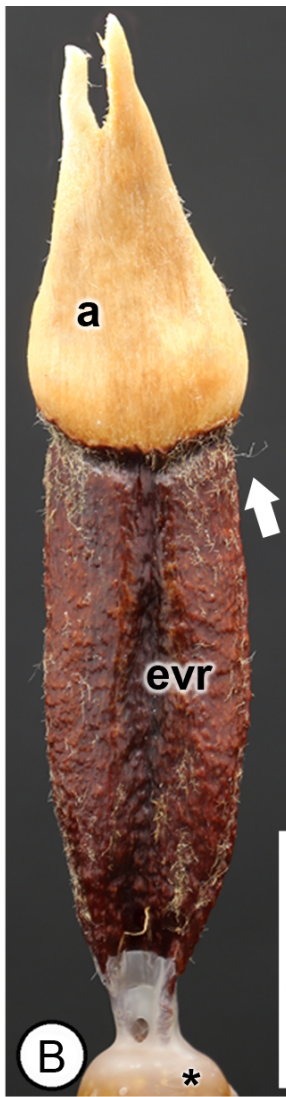
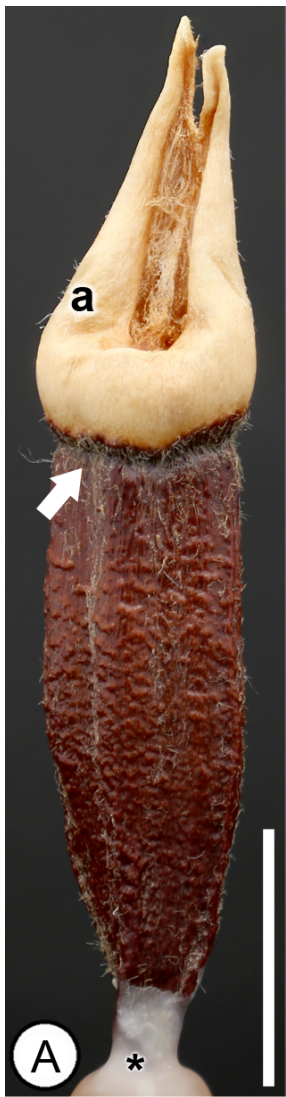


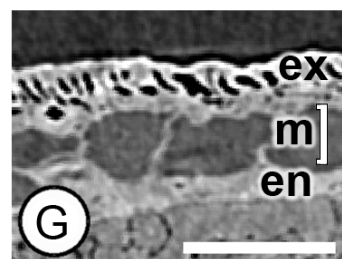
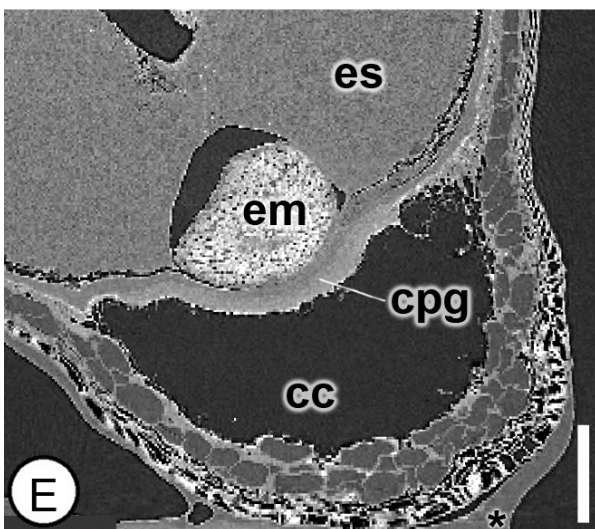
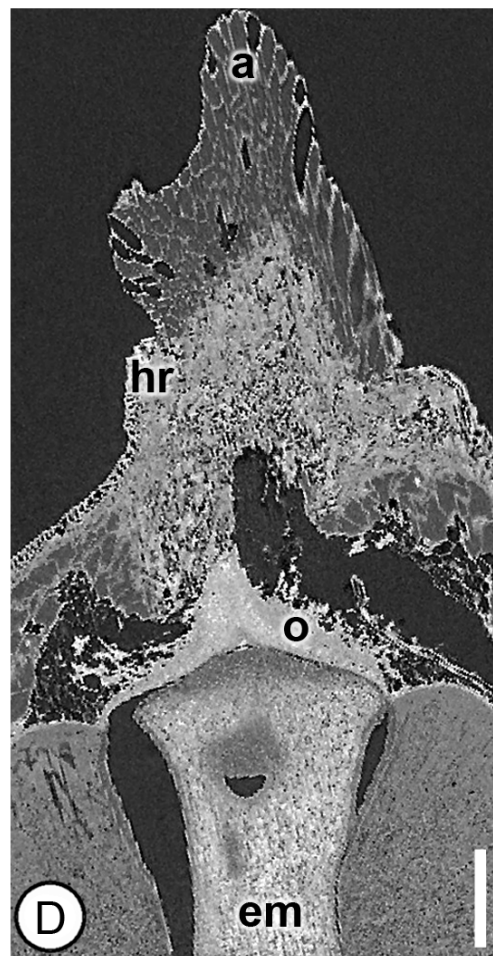
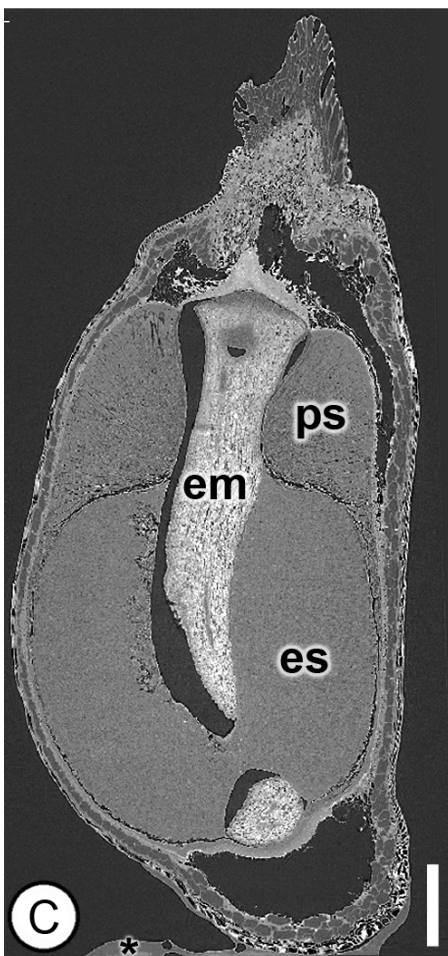


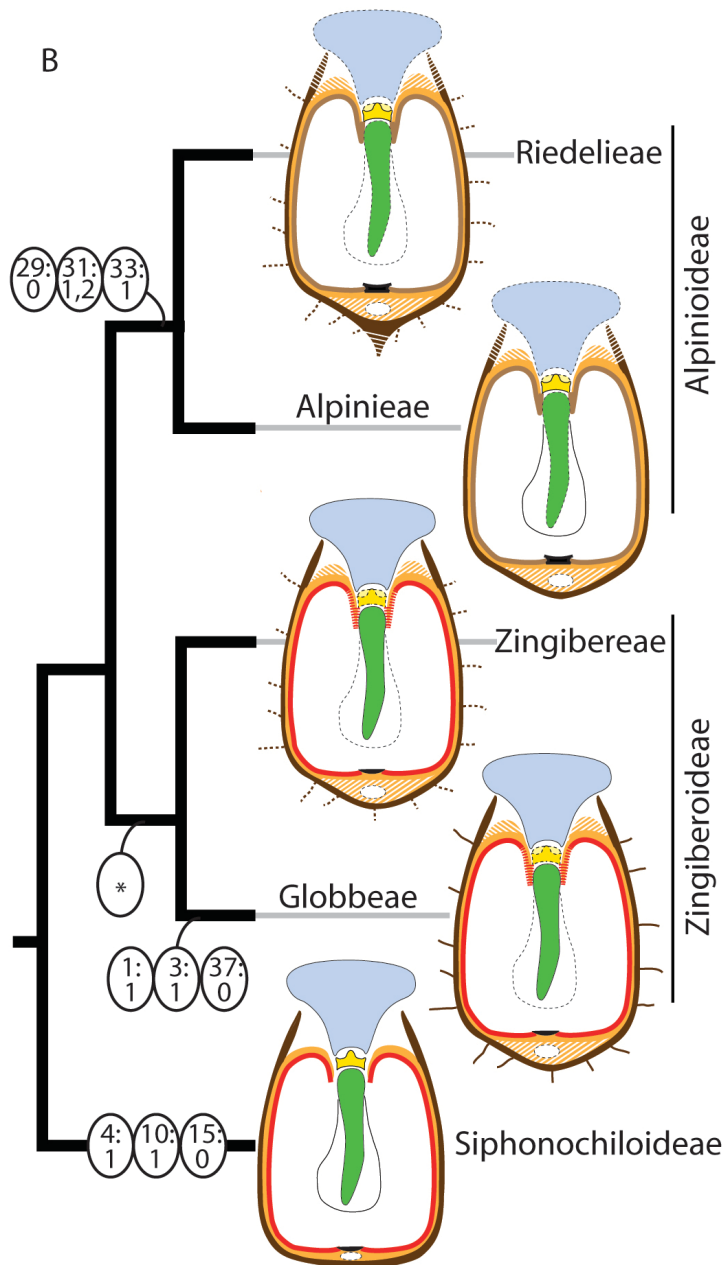
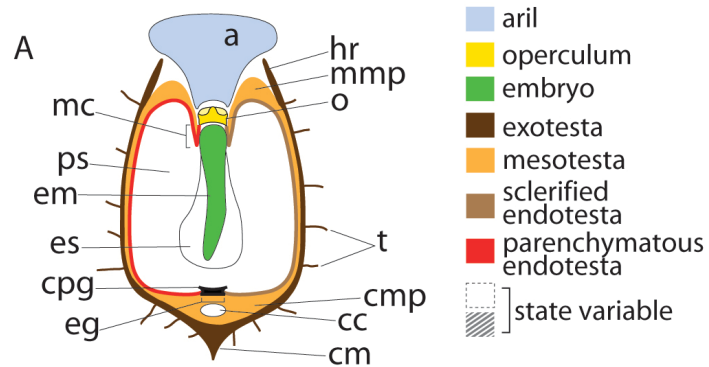






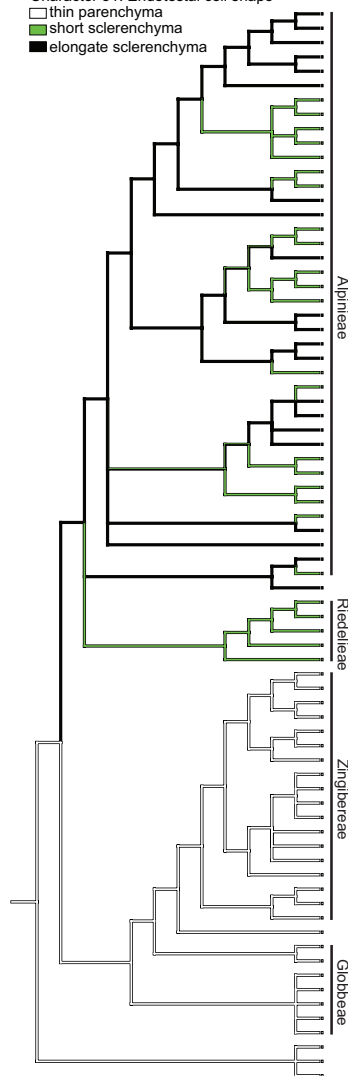






Character 31: Endotestal cell shape

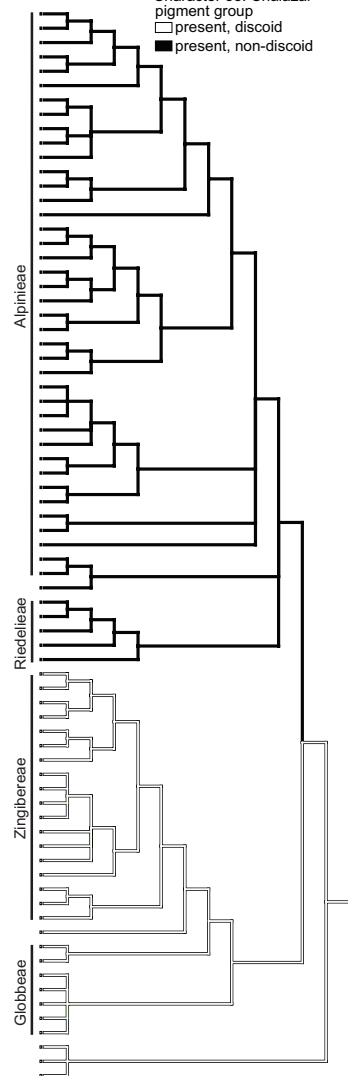
- thin parenchyma
- short sclerenchyma
- elongate sclerenchyma



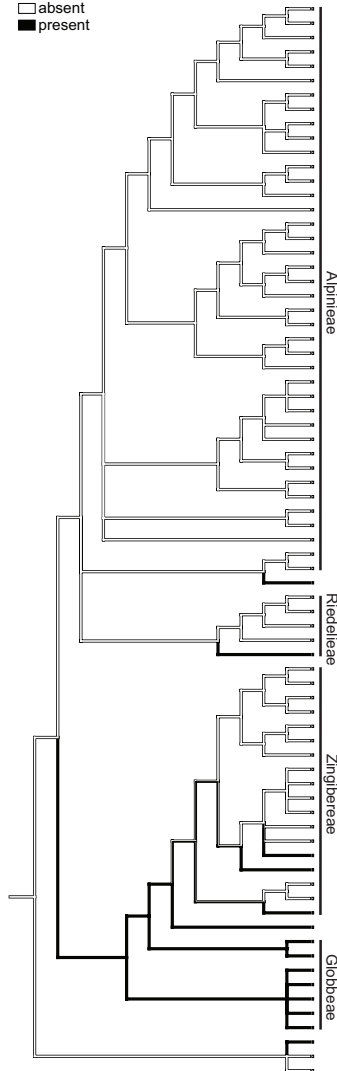
- Etingera yunnanensis*
- Etingera linguiformis*
- Etingera elatior*
- Hornstedtia scottiana*
- Hornstedtia leonurus*
- Hornstedtia conica*
- Alpinia purpurata*
- Alpinia oceanica*
- Vanoverberghia sepulchrei*
- Alpinia luteocarpa*
- Alpinia caerulea*
- Amomum ochreum*
- Amomum lappaceum*
- Amomum koenigii*
- Geostachys densiflora*
- Renealmia occidentalis*
- Renealmia lucida*
- Alpinia fax*
- Aframomum melegueta*
- Aframomum chrysanthum*
- Aframomum daniellii*
- Eleitaropsis unifolia*
- Amomum sericeum*
- Alpinia galanga*
- Alpinia conchigera*
- Alpinia nigra*
- Alpinia zerumbet*
- Alpinia malaccensis*
- Alpinia haenkei*
- Alpinia stachyodes*
- Alpinia japonica*
- Alpinia brevibrans*
- Alpinia aquatica*
- Plagiostachys philippinensis*
- Plagiostachys escritorii*
- Alpinia carolinensis*
- Alpinia boia*
- Geocharis aurantiaca*
- Alpinia rafflesiana*
- Alpinia javanica*
- Siliquamomum tonkinense*
- Riedelia sp.*
- Riedelia corallina*
- Pleuranthodium sp.*
- Burbridgea stanantha*
- Siamanthus siliquosus*
- Hedychium muluense*
- Hedychium hasseltii*
- Hedychium gardnerianum*
- Hedychium coronarium*
- Caulleya spicata*
- Caulleya gracilis*
- Roscoeia alpina*
- Zingiber thorelii*
- Zingiber spectabile*
- Zingiber officinale*
- Zingiber larsenii*
- Distichochlamys citrea*
- Kaempferia pulchra*
- Boesenbergia curtisii*
- Newmania sp.*
- Curcuma pierreana*
- Curcuma montana*
- Camptandra ovata*
- Monolophus sikkimensis*
- Hemiorchis sp.*
- Gagnepainia harmandii*
- Globba spathulata*
- Globba sessiliflora*
- Globba pendula*
- Globba maculata*
- Globba aurea*
- Aulotandra trigonocarpa*
- Siphonochilus kirkii*
- Siphonochilus aethiopicus*

Character 33: Chalazal pigment group

- present, discoid
- present, non-discoid



Character 3: Trichomes on seed coat or aril
 absent
 present



- Etilingera yunnanensis*
- Etilingera linguiformis*
- Etilingera elatior*
- Hornstedtia scottiana*
- Hornstedtia leonurus*
- Hornstedtia conica*
- Alpinia purpurata*
- Alpinia oceanica*
- Vanoverberghia sepulchrei*
- Alpinia luteocarpa*
- Alpinia caerulea*
- Amomum ochreum*
- Amomum lappaceum*
- Amomum koenigii*
- Geostachys densiflora*
- Renealmia occidentalis*
- Renealmia lucida*
- Alpinia fax*
- Aframomum melegueta*
- Aframomum chrysanthum*
- Aframomum daniellii*
- Eleitaropsis unifolia*
- Amomum sericeum*
- Alpinia galanga*
- Alpinia conchigera*
- Alpinia nigra*
- Alpinia zerumbet*
- Alpinia malaccensis*
- Alpinia haenkei*
- Alpinia stachyodes*
- Alpinia japonica*
- Alpinia brevibrans*
- Alpinia aquatica*
- Plagiostachys philippinensis*
- Plagiostachys escritorii*
- Alpinia carolinensis*
- Alpinia boia*
- Geocharis aurantiaca*
- Alpinia rafflesiana*
- Alpinia javanica*
- Siliquamomum tonkinense*
- Riedelia sp.*
- Riedelia corallina*
- Pleuranthodium sp.*
- Burbridgea stanantha*
- Siamanthus siliquosus*
- Hedychium muluense*
- Hedychium hasseltii*
- Hedychium gardnerianum*
- Hedychium coronarium*
- Caulleya spicata*
- Caulleya gracilis*
- Roscoeia alpina*
- Zingiber thorelii*
- Zingiber spectabile*
- Zingiber officinale*
- Zingiber larsenii*
- Distichochlamys citrea*
- Kaempferia pulchra*
- Boesenbergia curtisii*
- Newmania sp.*
- Curcuma pierreana*
- Curcuma montana*
- Camptandra ovata*
- Monolophus sikkimensis*
- Hemiorchis sp.*
- Gagnepaina harmandii*
- Globba spathulata*
- Globba sessiliflora*
- Globba pendula*
- Globba maculata*
- Globba aurea*
- Aulotandra trigonocarpa*
- Siphonochilus kirkii*
- Siphonochilus aethiopicus*

Character 15: Micropylar collar
 absent
 present

